



1 Comparing SWAT with SWAT-MODFLOW hydrological simulations when assessing
2 the impacts of groundwater abstractions for irrigation and drinking water

3 Wei Liu¹, Seonggyu Park^{2,3}, Ryan T. Bailey², Eugenio Molina-Navarro^{1,4}, Hans Estrup Andersen¹,
4 Hans Thodsen¹, Anders Nielsen¹, Erik Jeppesen¹, Jacob Skødt Jensen⁵, Jacob Birk Jensen^{6,7} and
5 Dennis Trolle¹.

6 ¹Department of Bioscience, Aarhus University, Silkeborg, Denmark;

7 ²Department of Civil and Environmental Engineering, Colorado State University, Fort Collins,
8 Colorado, USA;

9 ³Blackland Research & Extension Center, Texas A&M AgriLife, Temple, United States;

10 ⁴Department of Geology, Geography and Environment, University of Alcalá. Alcalá de Henares,
11 Madrid, Spain.

12 ⁵NIRAS, Aarhus, Denmark;

13 ⁶Department of Civil Engineering, Aalborg University, Aalborg, Denmark;

14 ⁷WatsonC, Aalborg, Denmark.

15 Correspondence: Wei Liu (weli@bios.au.dk, liuwei.alan@gmail.com)

16 Key Points:

- 17 • We compared the performance of SWAT and SWAT-MODFLOW and assessed the simulated
18 streamflow signals in response to a range of groundwater abstraction scenarios targeted for
19 irrigation and drinking water.
- 20 • The SWAT-MODFLOW complex was further developed to enable the application of the Drain
21 Package and an auto-irrigation routine.
- 22 • A PEST-based approach was developed to calibrate the coupled SWAT-MODFLOW.
- 23 • The SWAT-MODFLOW model produced more realistic results on groundwater abstraction
24 effects on streamflow.

25



26 Abstract

27 Being able to account for temporal patterns of streamflow, the distribution of groundwater resources,
28 as well as the interactions between surface water and groundwater is imperative for informed water
29 resources management. We hypothesize that, when assessing the impacts of water abstractions on
30 streamflow patterns, the benefits of applying a coupled catchment model relative to a lumped semi-
31 distributed catchment model outweigh the costs of additional data requirement and computational
32 resources. We applied the widely used semi-distributed SWAT model and the recently developed
33 SWAT-MODFLOW model, which allows full distribution of the groundwater domain, to a Danish,
34 lowland, groundwater-dominated catchment, the Uggerby River Catchment. We compared the
35 performance of the two models based on the observed streamflow and assessed the simulated
36 streamflow signals of each model when running four groundwater abstraction scenarios with real wells
37 and abstraction rates. The SWAT-MODFLOW model complex was further developed to enable the
38 application of the Drain Package of MODFLOW and to allow auto-irrigation on agricultural fields and
39 pastures. Both models were calibrated and validated, and an approach based on PEST was developed
40 and utilized to enable simultaneous calibration of SWAT and MODFLOW parameters. Both models
41 demonstrated generally good performance for the temporal pattern of streamflow, albeit SWAT-
42 MODFLOW performed somewhat better. In addition, SWAT-MODFLOW generates spatially explicit
43 groundwater-related outputs, such as spatial-temporal patterns of water table elevation. In the
44 abstraction scenarios analysis, both models indicated that abstraction for drinking water caused some
45 degree of streamflow depletion, while abstraction for auto-irrigation led to a slight total flow increase
46 (but a decrease of soil or aquifer water storages, which may influence the hydrology outside the
47 catchment). In general, the simulated signals of SWAT-MODFLOW appeared more plausible than
48 those of SWAT, and the SWAT-MODFLOW decrease in streamflow was much closer to the actual
49 volume abstracted. The impact of drinking water abstraction on streamflow depletion simulated by
50 SWAT was unrealistically low, and the streamflow increase caused by irrigation abstraction was
51 exaggerated compared with SWAT-MODFLOW. We conclude that the further developed SWAT-
52 MODFLOW model calibrated by PEST had a better hydrological simulation performance, wider
53 possibilities for groundwater analysis, and much more realistic signals relative to the semi-distributed
54 SWAT model when assessing the impacts of groundwater abstractions for either irrigation or drinking
55 water on streamflow; hence, it has the potential to be a useful tool in the management of water
56 resources in groundwater-affected catchments. However, this comes at the expense of higher
57 computational demand and more time consumption.



58 1. Introduction

59 The interaction between groundwater and surface water is an important aspect of the water cycle, and
60 the management or use of one often impacts the availability and temporal patterns of the other.
61 Improper management and over-exploitation of these water resource components influence the
62 sustainability of both the water resource itself and also the ecosystems that it supports. Groundwater
63 abstraction can cause a decline of the water table, and it thereby directly affects surface water bodies
64 connected to the aquifer (Jeppesen et al., 2015; Vainu and Terasmaa, 2016; Stefania et al., 2018). For
65 rivers in which a considerable portion of the streamflow is base flow, this can have a strong influence
66 on the general flow and deteriorate the function of river ecosystems (Johansen et al., 2011; Pardo and
67 Garcia, 2016). However, interactions between groundwater and surface water are difficult to observe
68 and measure, and it is, therefore, difficult to determine how much of the reduced streamflow recorded
69 in some rivers is due to abstractions and how much is due to natural weather-induced variability in
70 water table elevation.

71 For quantitative assessment of the impacts of pumping wells on streamflow, a hierarchy of modeling
72 tools has been developed, ranging from analytical models based on simple water balance equations to
73 regional, three-dimensional numerical models, depending on the complexity and available data source
74 of the site (Chen and Yin, 2001; Parkin et al., 2007; May and Mazlan, 2014). Analytical models generally
75 require less data for parameter identification and may therefore be applied when available data are
76 sparse, thus offering water managers a simple approach for estimating streamflow depletion with less
77 time, expertise, and financial costs (Glover and Balmer, 1954; Hunt, 1999; Huang et al., 2018; Zipper
78 et al., 2018). Nevertheless, as they do not simulate many of the physical processes and ignore the real-
79 world complexity, they may render unrealistic results. In contrast, numerical, process-based models
80 consider the entire complexity and heterogeneity of river-aquifer systems. Such models can simulate
81 the regional groundwater dynamics as well as the interactions between groundwater and surface water.
82 They are therefore part of local water management applications including estimation of streamflow
83 depletion, although they are generally more time-consuming and costly to set up, calibrate, test, and
84 apply.

85 MODFLOW is a physically-based, fully-distributed, and three-dimensional (3D) finite-difference
86 groundwater model, and it is considered a state-of-the-art international standard for simulating and
87 predicting groundwater conditions (<http://water.usgs.gov/ogw/modflow/>). It can be used to simulate
88 both steady state and transient conditions. MODFLOW outputs include groundwater hydraulic head
89 or drawdown at the center of each grid cell as well as groundwater flow rates to/from each stream



90 segment if the River (RIV) Package or the Streamflow Routing Package (SFR) is used (Wei et al.,
 91 2018). A number of studies have applied MODFLOW to assess the impact of groundwater abstraction
 92 on surface water resources (Sanz et al., 2011; May and Mazlan, 2014; Shafeeque et al., 2016; Stefania
 93 et al., 2018). However, MODFLOW does not simulate surface processes such as land-atmosphere
 94 interactions, agricultural management practices, and surface runoff (Lachaal et al., 2012; Surinaidu et
 95 al., 2014). To obtain spatial-temporal varying recharge rates, MODFLOW is therefore often linked
 96 with land-surface models such as the Precipitation-Runoff Modelling system (Markstrom et al., 2008;
 97 Markstrom et al., 2015) and the Soil and Water Assessment Tool (SWAT) (Izady et al., 2015; Wei et
 98 al., 2018).

99 The SWAT model is a semi-distributed catchment-scale model and has been widely used to simulate
 100 surface runoff, sediment erosion, pesticide and microorganism transport, and nutrient cycling in
 101 catchments at different geographical locations and scales (Nielsen et al., 2013; Fukunaga et al., 2015;
 102 Malago et al., 2017; Liu et al., 2019). In SWAT, the basin is divided into subbasins through a
 103 topography-based delineation, each subbasin containing a tributary of the river. Each subbasin is
 104 further divided into Hydrologic Response Units (HRUs), which are unique combinations of land use,
 105 soil type, and surface slope. When simulating hydrological dynamics, the areas of the HRUs are
 106 lumped within each subbasin, which makes SWAT computationally very efficient, but this comes at
 107 the expense of losing the spatial discretization of HRUs within a subbasin. SWAT has been utilized to
 108 simulate and quantify the groundwater resources (Ali et al., 2012; Cheema et al., 2014; Shafeeque et
 109 al., 2016) or the effects of drinking water or irrigation pumping on streamflow (Güngör and Göncü,
 110 2013; Lee et al., 2006). However, the SWAT model has traditionally emphasized surface processes as
 111 the model only includes a relatively simple representation of groundwater dynamics, and its output
 112 does not give any spatially explicit information on the groundwater table. In the most recent version
 113 of SWAT (v. 670), groundwater is represented by a lumped module in individual subbasins divided
 114 into a shallow and a deep aquifer. Both the shallow and the deep aquifer may contribute to streamflow
 115 as baseflow through a linear reservoir approximation, ignoring distributed parameters such as
 116 hydraulic conductivity and storage coefficients (Kim et al., 2008). With this simplified implementation
 117 of groundwater dynamics in SWAT, the model can mislead evaluation of groundwater resources or
 118 perform rather poorly in catchments where the streamflow is strongly dependent on groundwater
 119 discharge (Gassman et al., 2014).

120 To the best of our knowledge, there are two main approaches for making SWAT perform better in
 121 groundwater-dominated catchments. One approach is to modify the SWAT groundwater module code



122 itself. For example, (Zhang et al., 2016) modified the subroutines in the SWAT source code by
 123 converting the shallow aquifer water storage change into water table fluctuation with three
 124 groundwater parameters added, namely specific yield, the bottom bed burial depth, and shallow aquifer
 125 porosity. The modified SWAT could then simulate both water table fluctuations and water storage of
 126 the shallow aquifer in time and space. However, it still applied a lumped, linear reservoir approach to
 127 simulate groundwater storage and derive the water table at HRU level, which could give rise to errors
 128 as the HRUs are not spatially explicit within a subbasin. (Pfannerstill et al., 2014) implemented a three-
 129 storage concept in the groundwater module by splitting the shallow aquifer into a fast and a slow
 130 contributing aquifer. (Nguyen and Dietrich, 2018) replaced the deep aquifer in the original SWAT
 131 model with the multicell aquifer model. In both of these studies, the modified SWAT model achieved
 132 a better prediction of baseflow than the original SWAT model. However, both models only improved
 133 a part of aquifer system simulation, either the shallow aquifer or the deep aquifer. In addition, they
 134 maintained the semi-distributed approach.

135 The other approach for improving the performance of SWAT in groundwater-dominated catchments
 136 is to couple SWAT with a physically based, spatially distributed numerical groundwater model, such
 137 as MODFLOW. There are a few studies that have tried to integrate SWAT and MODFLOW code into
 138 one model complex (Kim et al., 2008; Yi and Sophocleous, 2011; Guzman et al., 2015; Bailey et al.,
 139 2016). The most recent of these, the SWAT-MODFLOW code developed by (Bailey et al., 2016)
 140 couples the most recent SWAT code with the MODFLOW-NWT code (a Newton-Raphson
 141 formulation for MODFLOW-2005 (Niswonger et al., 2011), which improves the solution of
 142 unconfined groundwater-flow problems). This coupled version has several advantages over others: an
 143 efficient HRU-grid cell mapping scheme (including generation of geographically explicit HRUs), the
 144 ability to use SWAT and MODFLOW models of different spatial coverage, the use of the
 145 MODFLOW-NWT code, public availability, and a graphical user interface that has been recently
 146 developed for its application (Bailey et al., 2017; Park et al., 2018). Recently, the current published
 147 SWAT-MODFLOW code (Version 2 on the SWAT website) has been applied to catchments in the
 148 USA (Bailey et al., 2016; Abbas et al., 2018; Gao et al., 2019), Canada (Chunn et al., 2019), Denmark
 149 (Molina-Navarro et al., 2019), Iran (Semiromi and Koch, 2019), and Japan (Sith et al., 2019). It has
 150 also been further developed for application in large-scale mixed agro-urban river basins (Aliyari et al.,
 151 2019). Within the coupled SWAT-MODFLOW framework, SWAT simulates surface hydrological
 152 processes, whereas MODFLOW-NWT simulates groundwater flow processes and all associated
 153 sources and sinks on a daily time step. In addition, the HRU-calculated deep percolation from SWAT
 154 is passed to the grid cells of MODFLOW as recharge, and MODFLOW-calculated groundwater-



155 surface water interaction fluxes are passed to the stream channels of SWAT. Hence, the model complex
156 accounts for two-way interactions between groundwater and surface waters and thereby enables a
157 potentially much better representation and thus understanding of the spatial-temporal patterns of
158 groundwater-surface water interactions, which are of key importance to catchment management in
159 groundwater-dominated catchments.

160 In Denmark, approximately 800 million m³ of water are abstracted annually and used for irrigation or
161 drinking water (GEUS, 2009), making the country highly dependent on groundwater. Since the very
162 dry summers in 1975 and 1976 led to dry out of many watercourses around some cities in Denmark,
163 the national government has endeavored to regulate the abstraction of surface and groundwater to a
164 level preventing negative impacts on in-stream biota. Gradually, direct abstraction from surface waters
165 has been prohibited and groundwater abstraction is regulated to secure a certain minimum flow in all
166 Danish rivers, mainly by moving the abstraction wells away from riverbanks and wetlands and
167 implementing a groundwater abstraction permit authority system. However, there still remains some
168 areas where groundwater exploitation is above the sustainable yield and causes streamflow depletion
169 according to the national water resource model (Henriksen et al., 2008).

170 To better understand how abstraction wells used for drinking water or irrigation may influence nearby
171 streamflow, we applied both SWAT and SWAT-MODFLOW to a lowland catchment in Northern
172 Denmark – the Uggerby River Catchment. We hypothesize that, when assessing impacts of water
173 abstractions on streamflow patterns, the benefits of applying SWAT-MODFLOW relative to SWAT
174 outweigh the costs of additional data requirements and computational resources. We compared the
175 performance of the two models and assessed the simulated signals of streamflow in a range of
176 groundwater abstraction scenarios with real wells and abstraction rates for either drinking water or
177 irrigation with both models. The SWAT-MODFLOW complex used in this study was further
178 developed based on the publically available version (<https://swat.tamu.edu/software/swat-modflow/>)
179 to enable application of the Drain Package of MODFLOW and to allow auto-irrigation. In addition, an
180 approach based on PEST (Doherty, 2018) was developed to calibrate the coupled SWAT-MODFLOW
181 by adjusting SWAT and MODFLOW parameters simultaneously against the observations of both
182 streamflow and groundwater table.

183

184



185 2. Materials and methods

186 2.1 Study area

187 The Uggerby River Catchment lies between latitude 57°17'10"- 57°35'25" N and longitude 9°58'47"-
 188 10°19'55" E. It covers an area of 357 km² and is located in the Municipality of Hjørring, which is
 189 situated in the northern part of Jutland, Denmark (Fig. 1). The Uggerby River originates from the
 190 southern part of Hjørring in Sterup and winds its way through the area of Hjørring, Sindal, Mosbjerg,
 191 Bindslev, and Uggerby and then discharges into the bay Tannisbugten at the coast of the North Sea.
 192 The study area has a typical Atlantic climate, which is temperate with an average annual temperature
 193 around 8 °C, being warmest in August (17 °C average) and coldest in January (0.5 °C average). The
 194 average annual precipitation during the study period 2002-2015 was approximately 933 mm with no
 195 obvious distinctions among seasons.

196 Figure 1.

197 The mean catchment elevation is 34.5 m a.s.l and ranges from 0 to 108 m. Land cover in the catchment
 198 is dominated by agricultural land, and the other land use types include evergreen forest, pasture,
 199 wetland, and urban areas. The soil types are loamy sand, sandy loam, and sand. The main crops grown
 200 in the area include winter wheat, winter rape, barley, corn, and grass. Artificial tile drains have been
 201 installed in parts of the agricultural land in the catchment, although the precise drainage locations are
 202 somewhat uncertain (Olesen, 2009). According to an investigation carried out by Hjørring
 203 Municipality in 2009, there are 101 drinking water pumping wells registered within the catchment and
 204 57 irrigation pumping wells placed on pasture and agricultural land. Generally, irrigation only occurs
 205 from April to October. The average annual irrigation amount varies from 80 to 200 mm depending on
 206 the types of crop and soil conditions (Aslyng, 1983).

207 2.2 Model set-up and coupling

208 2.2.1 SWAT model set-up

209 We used the QSWAT 1.5 interface (George, 2017), which works with the latest SWAT Editor version
 210 2012.12.19 and is integrated into a QGIS 2.8.1 interface. The input data for the SWAT model in this
 211 study include topography, land use, soil, climate, agricultural management, wells, and wastewater
 212 discharge as point sources.



213 The catchment was divided into 19 subbasins (Fig. 1) based on the 32 m pixel size Digital Elevation
 214 Model (DEM), which has been resampled from a 1.6 m LIDAR DEM (Knudsen and Olsen, 2008). For
 215 the creation of HRUs, we used the land use map based on the Danish Area Information System (NERI,
 216 2000) and the soil map based on a national three-layer soil map with a 250 m grid resolution (Greve
 217 et al., 2007), and surface slope type was classified into three classes ($<2\%$, $2-6\%$, $>6\%$). To reduce the
 218 number of HRUs and facilitate the posterior model linkage process, land use for range-grasses and
 219 range-brush, which covered only 1.3% and 1.9% of the total catchment area, respectively, were merged
 220 into pasture, and water (0.9%) was merged into wetland areas. In order to represent the agricultural
 221 management practices in detail, the agricultural area was split into three equally sized types with
 222 different five-year crop rotation schedules (Table 1) based on the real contour of agricultural field plots
 223 and the land use map. Similar to land use, soil types covering a minor part of the catchment (1% or
 224 less) were merged into similar soil types. The distribution and proportion of each land use, soil type,
 225 and slope band after reclassification are shown in Fig. 2. Based on the combination of land use, soils,
 226 and slope, the catchment was discretized into 2620 HRUs.

227 **Figure 2.**

228 Climate data used in the model comprised the 10 km-grid national daily precipitation data (six stations
 229 inside the catchment), 20 km-grid daily solar radiation and wind speed data (five stations inside or near
 230 the catchment), gauged-level daily maximum and minimum temperatures, and relative humidity data
 231 (one station, 27 km from the catchment) during 1997-2015 from the Danish Meteorological Institute
 232 (Lu et al., 2016).

233 Farm type and manure/mineral fertilizer application of each agricultural rotation as well as dates of
 234 sowing, harvesting, and tillage were assigned based on reported statistics for 2005 available from
 235 <http://www.dst.dk/en> (Table 1). We do not know the specific tile drain distribution within the entire
 236 catchment. In general, loamy soils in relatively flat areas are known to be tile drained in Denmark
 237 (Olesen, 2009). To represent this situation, tile drains were set up in agricultural land with a slope less
 238 than 2% and for soil types with a clay content above 8% (Thodsen et al., 2015), representing 27% of
 239 the agricultural land in the catchment.

240 We assumed that irrigation only occurs in the HRUs where irrigation pumping wells exist (based on a
 241 MODFLOW model created by NIRAS A/S). It is difficult to know the exact dates and water amount
 242 used for irrigation. Thus, to simulate the irrigation, auto-irrigation management was set up based on
 243 heat unit scheduling for the HRUs containing irrigation pumping wells. For the auto-irrigation of crops,



the water resource used for pumping was defined as the shallow aquifer, and the soil water content, commonly used as an indicator in actual field irrigation (Chen et al., 2017), was selected as the water stress identifier with 70 mm as the initial water stress threshold. With the number and location of pumping wells as well as their pumping rates obtained from the Well Package in the MODFLOW model, the water abstraction amounts from drinking water wells were added up in each subbasin and set as the water use pumped from the shallow aquifer in SWAT.

The only significant point source of the study area is the discharge from the wastewater treatment plant in Sindal located in subbasin 16. With a few other minor sources aggregated to a total discharge from the wastewater treatment plant, a total of 2768.8 m³ of water was discharged into the stream per day (data is based on an average for the period 2007-2010).

2.2.2 MODFLOW-NWT model set-up

A steady-state version of the MODFLOW-NWT model has previously been set up for the entire Hjørring Municipality, covering an area of 930 km², in which the Uggerby River Catchment is situated (Fig. 3). The model set-up was firstly established in 2011 and then updated in 2016 by the consultant company NIRAS A/S and Hjørring Water Supply Company, and has been applied for water resources management in the Hjørring Municipality. In the model set-up, the geology is represented by 5 hydro-stratigraphic layers, discretized into 183,112 grids (376 rows and 487 columns) with a discretization of 100 x 100 meters. The uppermost layer is unconfined and the remaining four layers are confined. The Upstream Weighting (UPW) Package for MODFLOW, which contains hydraulic properties of each cell, was used as the internal flow package, and a number of boundary condition packages, including Time-variant specified-head Package, Drain Package, River Package, Well Package, and Recharge Package, were employed in the model to simulate external stresses. The steady-state model was calibrated using 1,063 head observations sampled during the period 1996-2010 at 1,006 well locations distributed within the first, third, and fifth layer by a combination of manual calibration and auto-calibration through PEST (<http://www.pesthomepage.org/>).

Figure 3.

Eighteen different hydraulic conductivity values exist in the originally calibrated MODFLOW model. In order to facilitate the posterior SWAT-MODFLOW calibration, we reclassified and grouped the specific hydraulic conductivities into five groups. The grouping was made for grid cells of similar specific hydraulic conductivities, representing the sedimentary materials of clay, silt, silty sand,



274 mixture of silty sand and clean sand, and clean sand, respectively. Each group was assigned a unique
 275 specific hydraulic conductivity, which could be targeted for calibration.

276 For the SWAT-MODFLOW set-up, we converted the modified calibrated steady-state model into a
 277 transient model by assigning values to the specific yield (only for the unconfined layer) and specific
 278 storage of each cell according to the type of sedimentary materials of the cell and representative values
 279 of storage coefficients. The simulated heads generated by the steady-state model were used as the
 280 initial head conditions for the transient model.

281 **2.2.3 SWAT-MODFLOW coupling**

282 SWAT and MODFLOW were combined using the coupling framework developed by (Bailey et al.,
 283 2016) and following the procedures described in the instructions available from the SWAT website
 284 (<http://swat.tamu.edu/software/swat-modflow/>).

285 For this study, the following changes were made to the original SWAT-MODFLOW code: (1) the grid
 286 cells in the Drain Package were linked with SWAT subbasins so that groundwater removed from
 287 subsurface drains is routed to stream channels; and (2) groundwater pumping in agricultural areas or
 288 pastures is dictated by irrigation applied to HRUs through SWAT's auto-irrigation routines. For the
 289 latter, this is achieved by calculating the daily volume of applied irrigation water (irrigation depth *
 290 HRU area) and then extracting this volume from the underlying grid cells using MODFLOW's Well
 291 Package (Fig. 4). When applying the Drain Package of MODFLOW, the original tile drain routine in
 292 SWAT was disabled. The steps in the coupling procedure included: 1) disaggregation of HRUs to
 293 disaggregated hydrologic response units (DHRUs) through GIS processing to make the model spatially
 294 explicit; and 2) creation of six linking text files (HRUs to DHRUs, DHRUs to MODFLOW grids,
 295 MODFLOW grids to DHRUs, MODFLOW river cells to SWAT subbasin rivers, MODFLOW drain
 296 cells to subbasin rivers, irrigation pumping wells in HRUs to MODFLOW grids) through GIS
 297 processing. All related files (MODFLOW input files, original SWAT model files, linkage files) were
 298 stored in one working directory for SWAT-MODFLOW execution.

299 **Figure 4.**

300 **2.3 Model calibration**

301 **2.3.1 SWAT calibration**



302 The Sequential Uncertainty Fitting Algorithm (SUFI2), which is implemented in the SWAT-CUP
 303 software (Abbaspour, 2015), was used to calibrate discharge performance in SWAT. The latest
 304 SWAT-CUP version (5.1.6.2) was used. Calibration was performed based on daily discharge records
 305 from 1 Jan. 2002 to 31 Dec. 2008, with a previous 5-year model warm-up period and using Nash-
 306 Sutcliffe efficiency (N_{SE}) as the objective function. Five parameters at basin-wide level and 17
 307 parameters at subbasin level related to streamflow were selected and assigned initial calibration value
 308 ranges based on expert judgement and previous SWAT applications in Danish catchments (Lu et al.,
 309 2015; Molina-Navarro et al., 2017).

310 In the study area, two hydrologically connected monitoring stations are found, located at the outlet of
 311 subbasin 13 (station A) and subbasin 18 (station B), respectively (Fig. 1). The two stations represent a
 312 small (average discharge $1.95 \text{ m}^3 \text{ s}^{-1}$) and relatively large (average discharge $4.56 \text{ m}^3 \text{ s}^{-1}$) stream in
 313 Denmark, and both were used for calibration and validation in this study. Station A is located upstream
 314 from station B and its flow therefore has an influence on station B. Thus, the simulated discharge of
 315 station A was preliminarily calibrated first (initial range of related parameters are shown in Table 2),
 316 running 3 iterations with 500 simulations each. After the final iteration for station A, the subbasin level
 317 parameters for the area upstream station A were fixed, while the final ranges of the basin-wide
 318 parameters were used in the subsequent calibration of station B. As the basin-wide parameter values
 319 can impact the hydrology of the entire catchment, for the calibration of station B, discharge data from
 320 both station A and B were included in the objective function. An additional three iterations with 500
 321 simulations were run, where the subbasin level parameters for the remaining area upstream station B
 322 were calibrated using the same initial parameter range as for station A (Table 2), while the basin-wide
 323 parameter ranges from the final calibration step for station A were used as initial ranges. By this
 324 approach, we attempted to make the basin-level parameters representative for both upstream and
 325 downstream areas. Afterwards, the water stress threshold was calibrated manually to ensure proper
 326 simulation of the annual irrigation amount, which ranges from $80 \text{ to } 120 \text{ mm yr}^{-1}$ and occurs in the
 327 period April to October (Aslyng, 1983). Once the calibration was completed and the parameters were
 328 fixed, we validated the model by running one simulation from 1 Jan. 1997 to 31 Dec. 2015 using the
 329 first 12-years as a warm-up period.

330 To analyze parameter sensitivity and make the sensitivity analysis comparable with SWAT-
 331 MODFLOW, an additional iteration with 500 simulations was run for the calibration period. In this
 332 iteration, the ranges of basin level parameters and subbasin level parameters for the area upstream
 333 station A were the same as those in the final calibration step for station A, while the ranges of subbasin



level parameters for the area upstream station B were identical with the final calibration step for station B.

Table 2.

2.3.2 SWAT-MODFLOW calibration

After model coupling, the SWAT-MODFLOW was calibrated by adjusting SWAT and MODFLOW parameters simultaneously against the observations of both streamflow and groundwater table through a combination of manual calibration and auto-calibration by the widely used PEST approach (Doherty, 2018). The periods used for model warm-up, calibration, and validation were identical to those used for SWAT. SWAT-MODFLOW can also be run through SWAT-CUP, whereby the summary statistics of model performance can be derived and directly compared between SWAT and SWAT-MODFLOW. In addition, model.in and Swat_Edit.exe, which are included in the creation of the SWAT-CUP project folder, can be used to adjust SWAT parameters within the PEST routine.

The framework using PEST to calibrate SWAT-MODFLOW was firstly introduced by (Park, 2018). We applied this framework to this study as well but with BEOPEST (Doherty, 2018) instead of PEST as the PEST executable file. Figure 5 presents a schematic diagram illustrating how PEST is utilized for the SWAT-MODFLOW calibration in this study. Five types of files are required to run PEST: PEST control file, PEST executable file, model batch file, model input template files, and model output instruction files. The PEST control file is a master file that contains control variables, initial values and ranges of model parameters, observations and their weights for deriving the value of the objective function, as well as names of all input and output files related to calibration. BEOPEST was used as the PEST executable file that enables parallelization of model runs on multiple computer cores, thereby shortening the calibration time considerably. After each iteration of a PEST run, the PEST optimization algorithm adjusts the model parameter values to optimize the value of the objective function. The newly updated model parameter values are then written to model input files using input template files and Swat_Edit.exe. Next, the SWAT-MODFLOW executable is called by a batch file and generates a set of output files if the model runs successfully. A python script (exsimvalue.py) extracts the simulated values from the streamflow output file (output.rch) and the groundwater table output file (swatmf_out_MF_obs). The extracted simulated data are read by PEST using information from the model output instruction file and then compared against the corresponding observations. Each iteration includes a number of model runs according to the control variable set in the PEST control file to allow adjustment of parameter values. After each iteration, the objective function and a Jacobian matrix are



calculated, based on which the PEST will make its decision for the next iteration until one of its stopping criteria, specified in the PEST control file, is met. More detailed information about the optimization process and principles of PEST can be found in (Zhulu, 2010) and the PEST manual (Doherty, 2018).

Figure 5.

As shown in Table 3, 26 parameters from SWAT related to surface hydrological processes and 13 parameters from MODFLOW were selected and calibrated through PEST. For SWAT parameters, with the parameters related to tile drains and groundwater excluded, the final calibrated parameter values used in SWAT were applied as the initial values in PEST, and the parameter ranges used in the iteration for SWAT parameter sensitivity analysis were employed as the parameter ranges in PEST. By manually adjusting MODFLOW parameter values to test their impacts on model outputs, storage coefficients (SY and SS), horizontal hydraulic conductivity (HK), and two drain conductance (COND) were deemed as the potential sensitive parameters, with the value of HANI (the ratio of hydraulic conductivity along columns to hydraulic conductivity along rows) always being 1 and the values of VKA (the ratio of horizontal to vertical hydraulic conductivity) fixed as the values in the original MODFLOW set-up. For MODFLOW parameters, the originally calibrated and modified parameter values in the steady-state MODFLOW version were used as the initial parameter values in PEST, and a small range around the initial values was assigned as the parameter range according to the experience from manual calibration and representative values (derived from http://www.aqtesolv.com/aquifer-tests/aquifer_properties.htm).

Table 3.

The observed streamflow used for calibrating SWAT-MODFLOW was identical to that used for calibrating SWAT. Relatively continuous observations of the groundwater table were available at the location of two grid cells, and these were used for calibrating the variation of the groundwater table simulated by SWAT-MODFLOW. Because station A is located upstream from station B and its flow thus has an influence on station B, the weight for deriving the objective function for station A, which represents a small stream, was set to 2, and the weight for station B was set to 1. The weights for the two grid cells were set to 1.

In order to establish template files and facilitate the process of modifying parameter values (HK, SS, SY) in the UPW Package while running PEST, the parameter value file (PVAL) and Zone file



395 (<https://water.usgs.gov/ogw/modflow-nwt/MODFLOW-NWT-Guide/>) were first established based on
 396 the original UPW Package through running a code file in FORTRAN.

397 Ten iterations were specified as the stop criteria in the PEST control file. Due to the large number of
 398 grid cells (183,112) in the MODFLOW set-up and the amount of disaggregated HRUs (DHRUs,
 399 66,765) compared with the case study conducted by (Bailey et al., 2017), it takes the coupled SWAT-
 400 MODFLOW model complex around 4 hours to run a single simulation (12 years' simulation) when
 401 MODFLOW runs with a daily interval. To shorten the calibration time, 11 BEOPEST slaves were
 402 created on three computers with BEOPEST as the pest executable file so that 11 simulations could be
 403 run simultaneously. A total of 638 simulations were run before the stop criteria was achieved. With
 404 the calibrated parameters fixed, the water stress threshold was calibrated manually to ensure proper
 405 simulation of the annual irrigation amount (ranging from 80 to 120 mm yr⁻¹, occurring in the period
 406 between April to October) and make the simulated average annual irrigation amount in the irrigated
 407 HRUs (mm yr⁻¹) comparative with that in the calibrated SWAT model. Finally, the SWAT-
 408 MODFLOW model performance was validated following a procedure equivalent to that used for
 409 SWAT.

410 **2.4 Water abstraction scenarios**

411 Besides the 158 wells registered within the Uggerby River Catchment, another 256 wells exist outside
 412 the catchment but inside Hjørring Municipality (Fig. 3). All these wells were included in the Well
 413 Package in the SWAT-MODFLOW set-up. In SWAT-MODFLOW, the irrigation pumping source was
 414 defined as the third layer. For drinking water wells, 7 of the 101 drinking water wells were placed in
 415 the first layer, 91 in the third layer and 3 in the fifth layer. In order to evaluate the impacts of both
 416 irrigation and drinking water abstractions on streamflow for streams of difference sizes, four
 417 abstraction scenarios were designed and applied to the Uggerby River Catchment using both models:
 418 1) the no-wells scenario, where all abstractions are terminated; 2) the irrigation-wells-stop scenario,
 419 where all abstractions in irrigation wells are terminated, while abstractions in drinking water wells
 420 remain; 3) the drinking-wells-stop scenario, where all abstractions in drinking water wells are
 421 terminated, while abstractions in irrigation wells remain; and 4) the baseline scenario, where
 422 abstractions in all wells are included, which represents the current level of abstraction. We assumed
 423 that the point source discharge to the stream in subbasin 16 would remain the same in all scenarios.
 424 Once the scenarios were simulated, their impacts on streamflow were analyzed by assessing the
 425 average annual runoff amount, the contribution of water balance components, and the temporal



426 dynamics of streamflow. The simulated signals of SWAT and SWAT-MODFLOW in the abstraction
 427 scenarios were then compared.

428 **3 Results**

429 **3.1 Steady-state MODFLOW performance**

430 Visualization of the proximity of simulated and observed head contours (Fig. 6) was used to evaluate
 431 how well the modified calibrated MODFLOW model performed at steady state and three summary
 432 statistics were used as indicators for goodness of model fit (Table 4). The simulated heads and
 433 summary statistics have changed little compared with the original calibrated MODFLOW set-up. Thus,
 434 the modified calibrated MODFLOW model was satisfactory and suitable as a basis for coupling to
 435 SWAT in transient mode.

436 **Figure 6.**

437 **Table 4.**

438 **3.2 SWAT and SWAT-MODFLOW transient model performance**

439 The SWAT and SWAT-MODFLOW models both represented well the streamflow hydrographs during
 440 the calibration period, while during the validation period, one high peak flow event occurred in the
 441 SWAT and SWAT-MODFLOW simulations but not in the observations (Fig. 7). The baseflow was
 442 generally reproduced well by both models, but the SWAT-MODFLOW visibly performed better.

443 **Figure 7.**

444 **Table 5.**

445 Compared with the recommended evaluation criteria by (Moriassi et al., 2015), the statistical
 446 performance (Table 5) suggested “very good” performance of both models during the calibration
 447 period based on percent bias (P_{BIAS}). During the validation period, the models performed “good” at
 448 station A and “satisfactory” at station B. For N_{SE} values, the performance was “very good” for SWAT-
 449 MODFLOW calibration at station B, “good” for SWAT-MODFLOW calibration at station A,
 450 “satisfactory” for SWAT calibration and SWAT-MODFLOW validation at both stations and SWAT
 451 validation at station A, but “unsatisfactory” for SWAT validation at station B. For R^2 values, the



performance was “good” for SWAT-MODFLOW calibration, “satisfactory” for SWAT calibration and SWAT-MODFLOW validation, but “unsatisfactory” for SWAT validation.

The statistical performances of SWAT-MODFLOW with and without PEST calibration were compared. After calibration by PEST, the summary statistics of SWAT-MODFLOW were improved, especially for the validation period at station B where the performance increased from “unsatisfactory” to “satisfactory” according to N_{SE} values (Table 5). In addition, the weighted residuals between simulation and observation were reduced after calibration by PEST, with the reduced residuals mainly coming from streamflow simulation (Table 6).

Table 6.

In SWAT, almost all the top 12 sensitive parameters (Fig. 8) were surface process parameters (Table 2) except for the groundwater parameter GW_DELAY. In contrast, for SWAT-MODFLOW (Table 3), all the top 12 sensitive parameters were groundwater parameters with the exclusion of only one surface process parameter OV_N.

Figure 8.

Compared with SWAT, the SWAT-MODFLOW model not only produced output for streamflow but also for the groundwater table of each cell on any given day. The variation of groundwater heads across the simulation period was minimal for layer 1, while there was some, albeit small, variation in layer 3 (Fig. 9). There was generally a good agreement between the groundwater head level and dynamics simulated by SWAT-MODFLOW and that was recorded at the two observation wells within the catchment (Fig. 10).

Figure 9.

Figure 10.

For the water balance, the evaporation simulated by SWAT-MODFLOW was a little higher (13 mm yr^{-1}) than that simulated by SWAT, while the total water yields (total stream flow) simulated by SWAT and SWAT-MODFLOW were almost equal (Table 7). The water balance components, however, differed substantially. Compared with SWAT, the surface runoff simulated by SWAT-MODFLOW was a little higher, while the lateral subsurface flow and groundwater flow (simulated by the River Package) were much lower. In SWAT-MODFLOW, the largest contributor to streamflow was the



480 drain flow simulated by the Drain Package (constituting 70% of the streamflow). Conceptually,
 481 however, this can also be viewed as a surface-near groundwater contribution. Hence, when lumping
 482 the contribution from drains and groundwater, these are clearly the dominant sources for streamflow
 483 in both the SWAT and SWAT-MODFLOW model.

484 **Table 7.**

485 **3.3 Water abstraction scenarios simulation**

486 The annual abstractions by drinking water wells or irrigation wells set up in the two models were
 487 approximately equivalent (Table 8). In the SWAT simulations, compared with the no-wells scenario
 488 (scenario 1), a decrease in the average annual stream flow was observed in scenario 2 (only drinking
 489 water wells), while an increase was recorded in scenario 3 (only irrigation wells) and scenario 4 (both
 490 drinking water and irrigation wells). In the SWAT-MODFLOW simulations, the average annual
 491 streamflow decreased not only in scenario 2, but also in scenario 4, and at subbasin 18 outlet in
 492 scenario 3, while a slight increase occurred at subbasin 13 outlet in scenario 3. The decrease in scenario
 493 2 simulated by SWAT-MODFLOW was much larger than that by SWAT and also closer to the
 494 abstracted amount, and the increase at subbasin 13 outlet in scenario 3 simulated by SWAT-
 495 MODFLOW was apparently lower than that simulated by SWAT (Table 8).

496 **Table 8.**

497 In SWAT, the decrease of average annual total flow in scenario 2 was minimal as a result of a tiny
 498 decrease in the groundwater return flow (Fig. 11a). In scenario 3 and scenario 4, with unchanged tile
 499 flow, all the other flow components rose, especially groundwater and lateral soil discharge. In SWAT-
 500 MODFLOW, the decrease of average annual total flow in scenario 2 also resulted from a decreased
 501 groundwater return flow, but the decrease was much larger than that simulated by SWAT. In scenario
 502 3, the lateral soil runoff and drain flow increased in SWAT-MODFLOW similar to SWAT, while in
 503 scenario 4, reduced drain flow was recorded (Fig. 11b). Compared with the no-wells scenario, the
 504 amount of evapotranspiration remained unchanged in scenario 2, whereas it increased by 5 mm yr⁻¹
 505 in the scenarios with irrigation wells in both the SWAT and SWAT-MODFLOW simulations. In the
 506 scenario with only irrigation, evapotranspiration and total flow increased in both the SWAT and
 507 SWAT-MODFLOW simulations, but the soil or aquifer water storage decreased according to the water
 508 balance.



509 **Figure 11.**

510 When comparing the temporal patterns of streamflow with the no-wells scenario (scenario 1), we found
 511 the daily discharge difference in scenario 2 (only drinking water wells) to be almost always negative
 512 (sometimes zero), while in scenario 3 (only irrigation wells) and scenario 4 (both drinking water and
 513 irrigation wells) it fluctuated around zero in simulations by both SWAT and SWAT-MODFLOW (Fig.
 514 12). Thus, the daily flow in the scenario with drinking water wells was almost always lower than the
 515 scenario without drinking water wells, and the daily flow in the scenario with only irrigation wells or
 516 the scenario with both irrigation and drinking water wells could be higher or lower than the scenario
 517 without wells. The daily discharge difference between scenario 2 and the no-wells scenario simulated
 518 by SWAT-MODFLOW was obvious, but the difference using SWAT was minimal. In the comparison
 519 of scenario 3 with the no-wells scenario, when the discharge difference was positive after an irrigation
 520 event, it descended smoothly in the SWAT simulation and more sharply in the SWAT-MODFLOW
 521 simulations.

522 **Figure 12.**

523 In the SWAT-MODFLOW set-up, the water exchange between aquifer and streams occurs between
 524 each MODFLOW river/drain cell and its surrounding cells. The newly developed SWAT-MODFLOW
 525 model complex can output the daily rate of water exchange between aquifer and streams for each
 526 subbasin. When the water exchange is positive, it is indicative of water flow from the aquifer to the
 527 stream. The temporal pattern of groundwater discharge was the same as for the stream flow, and the
 528 temporal patterns of the differences in groundwater discharge between the abstraction scenarios and
 529 the no-wells scenario were similar to the differences in streamflow, except for some peak flow days
 530 (Fig. 13), which indicates that the abstraction-induced streamflow change followed the groundwater
 531 discharge change.

532 **Figure 13.**

533 **4. Discussion**

534 **4.1 Performance and parameter sensitivity of SWAT and SWAT-MODFLOW**

535 Both the SWAT and SWAT-MODFLOW model simulated the temporal patterns of streamflow
 536 generally well at the two hydrological stations during the calibration and validation periods. However,
 537 visually SWAT-MODFLOW performed better, especially during recession curves and low flow



538 periods, suggesting a better simulation of the interaction between surface water and groundwater.
 539 Accordingly, the corresponding summary performance statistics were also better for SWAT-
 540 MODFLOW. The simulated peak flow on 16 October 2014 by both models was much higher than the
 541 observed data (Fig. 7). This discrepancy may be attributed to a high record of precipitation on that day
 542 based on a 10 by 10 km grid, which may not be representative for the wider catchment. Additionally,
 543 it is also likely that the observed streamflow was underestimated as it is calculated from the Q-h
 544 relation, which typically does not adequately cover peak flow events (Poulsen, 2013).

545 In the parameter sensitivity analysis, the surface process parameters of the two models shared the same
 546 ranges, while the models had different groundwater modules and parameters. While the SWAT-
 547 MODFLOW calibration was based on an objective function that took into account not only streamflow
 548 but also groundwater heads at the location of two wells, the calibration by PEST mainly improved the
 549 streamflow simulation performance (Table 4). According to the parameter sensitivity ranking, the
 550 parameters regarding groundwater processes in SWAT-MODFLOW played an important role in the
 551 streamflow simulation performance, while in SWAT, the impact of groundwater module parameters
 552 on streamflow simulation was generally insignificant. This reflects the shortcoming of the SWAT
 553 groundwater module, which ignores the variability in distributed parameters such as hydraulic
 554 conductivity and storage coefficients, represents groundwater by a lumped module in individual
 555 subbasins, and contributes to the stream network as baseflow based on a linear reservoir approximation.
 556 With this simplified implementation of groundwater dynamics and water exchange between surface
 557 water and groundwater in SWAT, the discharge simulated by SWAT cannot be optimized to the same
 558 extent as that simulated by SWAT-MODFLOW.

559 The availability of spatial-temporal patterns of the groundwater head in SWAT-MODFLOW could
 560 significantly benefit groundwater resources management and provide yet another level of
 561 understanding of water resources dynamics within a catchment. The outputs of SWAT-MODFLOW
 562 in this study showed that the model performed well, not only in streamflow simulations but also with
 563 respect to the spatial-temporal patterns of the simulated groundwater head. In contrast, since no
 564 information of groundwater table output is provided by SWAT, its goodness in streamflow simulation
 565 may potentially be based on an improper groundwater simulation where its performance on
 566 groundwater simulation is unknown.

567 4.2 Models ability to simulate effects of groundwater abstractions on streamflow



568 In scenario 2 where only drinking water wells are active according to the water balance where there is
 569 no change in evaporation compared with the no-wells scenario, we expected that the streamflow
 570 depletion simulated by SWAT would be approximately equivalent to the abstracted water volume,
 571 taking into account a possible small change in the aquifer or soil storage. However, results in this study
 572 showed that the impact of drinking water abstractions on streamflow in the SWAT simulation was
 573 negligible. In the SWAT-MODFLOW set-up, because the aquifer in the Uggerby River Catchment is
 574 connected to and interactive with an area outside of the topographical catchment (Fig. 3), the
 575 abstraction from an aquifer located in the Uggerby River Catchment not only impacts the hydrology
 576 inside but potentially also outside the catchment. According to the water balance, we expected that the
 577 SWAT-MODFLOW simulated streamflow depletion in the catchment would be lower at a level
 578 somewhat equivalent to the abstracted water volume. With equivalent abstraction for drinking water,
 579 the annual flow decrease simulated by SWAT-MODFLOW was much larger than that by SWAT and
 580 closer to the abstracted volume. Therefore, we conclude that SWAT simulations underestimate the
 581 impacts of groundwater abstraction for drinking water on streamflow depletion, while SWAT-
 582 MODFLOW provided more realistic assessments.

583 The simulated irrigation operation abstracts water from an aquifer and then applies the water onto the
 584 surface of agricultural land or pasture. Most of the water infiltrates back into the soil and is then utilized
 585 by the vegetation and partly lost through evapotranspiration or infiltrates deeper to the aquifer, and a
 586 small part of the water might flow to streams directly as a small increase in surface runoff. Though the
 587 abstraction causes groundwater depletion, the recharge from the irrigated water can partly refill the
 588 aquifer and produce groundwater discharge. Since in the SWAT-MODFLOW set-up the aquifer in the
 589 Uggerby River Catchment was connected and interactive with an outside area, after each event of
 590 groundwater abstraction for irrigation, the aquifer storage would be recharged not only from the
 591 irrigated land area but also by the groundwater flowing from the outside area. If the recharge rate is
 592 larger than the abstracted water amount, the groundwater discharge to the stream will presumably
 593 increase. Hence, the irrigation events also brought about a slight increase of average annual stream
 594 flow at the subbasin 13 outlet (Table 8), and a slight total flow increase within the catchment (Fig.
 595 11b). The subbasin aquifers in the SWAT set-up are closed and have no interaction with areas outside
 596 a subbasin. Meanwhile, the abstracted amount of water from aquifers for irrigation is larger than the
 597 amount of returning aquifer recharge from irrigated water, and we would therefore expect decreasing
 598 groundwater discharge to streamflow in SWAT simulations. However, the SWAT simulations also
 599 showed that irrigation led to enhanced streamflow (Table 8, Fig. 11a), which apparently was even
 600 higher than the increase simulated by SWAT-MODFLOW. This supports the point mentioned above



601 that SWAT underestimates the abstraction effect on streamflow depletion. SWAT simulations can,
602 therefore, lead to incorrect assessments of the impacts of groundwater abstractions for irrigation on
603 streamflow, while SWAT-MODFLOW provided more realistic assessments.

604 Upon inspecting the SWAT source code, it appears that the groundwater discharge calculation
605 equation used in SWAT does not take into account the impact of water abstraction from shallow
606 aquifers on water table fluctuations. Thus, the groundwater removal by abstractions in the SWAT
607 simulation does not have a direct effect on the groundwater discharge, which may explain the
608 somewhat surprising simulation signals of SWAT. In addition, in the equation, the groundwater
609 discharge on the current day is highly related to the groundwater discharge on the previous day, and
610 the increase of the groundwater discharge resulting from each irrigation application could then lead to
611 enhanced groundwater discharge for several days in a row. This may explain why the increased
612 discharge following an irrigation event descended more smoothly in SWAT than in SWAT-
613 MODFLOW (Fig. 12).

614 In the SWAT-MODFLOW model, the exchange rate between groundwater and surface water is based
615 on the head difference between the river stage (or drain cell stage) and the head of its surrounding
616 groundwater grid cells. This can reflect the temporally dynamic hydrological processes and also the
617 impacts from all the external stressors (e.g. temporally and spatially varying recharge and groundwater
618 abstractions) on water table fluctuations. Naturally, this should also allow SWAT-MODFLOW to
619 provide more realistic assessments of the impacts of groundwater abstractions on streamflow in
620 comparison with SWAT.

621 While setting up the drinking water abstraction in SWAT, three limitations were identified, also
622 reported in (Molina-Navarro et al., 2019). The first is that SWAT only allows one decimal point for
623 abstraction numerical inputs with a unit of $10^4 \text{ m}^3 \text{ day}^{-1}$ for each month. This means that pumping rate
624 variations within one month cannot be simulated by SWAT and that the accuracy of abstraction
625 dynamics thus cannot be guaranteed. As a result of this limitation, the abstraction amount in SWAT
626 and SWAT-MODFLOW was not completely identical. The second limitation is that the abstraction
627 from deep aquifer did not result in any streamflow change. Therefore, all the abstraction sources had
628 to be defined as the shallow aquifer in SWAT to achieve a signal in streamflow despite that we had at
629 least three wells receiving water from a deep aquifer (the fifth layer according to the MODFLOW-
630 NWT set-up). The last limitation is that the abstraction rates of all wells in each subbasin in SWAT
631 have to be summed up to one input value, thereby ignoring the specific location of wells within
632 individual subbasins.



SWAT-MODFLOW overcomes the limitations in SWAT by exploiting the spatial explicitness of MODFLOW where groundwater abstraction can be simulated using the Well Package, which allows many decimal points for abstraction inputs as well as user-defined units, pumping rates at potentially daily intervals, and wells located in any vertical layer and any grid cell within a subbasin. In addition to the outputs from SWAT, SWAT-MODFLOW also provides fully distributed groundwater-related outputs such as spatial-temporal patterns of water table elevation, distributed aquifer recharge, and groundwater-surface water exchange rates at a cell level, permitting detailed analysis of groundwater and its interaction with surface water. This may be an important input to groundwater resources management (e.g. groundwater abstraction) and the solving of surface water rights issues. These capabilities demonstrate the advantage of SWAT-MODFLOW over modifying the SWAT groundwater module codes to improve groundwater flow simulation (Nguyen and Dietrich, 2018; Pfannerstill et al., 2014; Zhang et al., 2016), which remains a semi-distributed way to simulate subsurface hydrologic processes and does not generate detailed groundwater outputs. This point supports the findings about the advantages of SWAT-MODFLOW over SWAT in (Molina-Navarro et al., 2019) but using a much more complex set-up.

4.3 Performance of SWAT-MODFLOW and SWAT relative to other recent studies

In previous studies, after coupling a calibrated SWAT and calibrated MODFLOW model, the SWAT-MODFLOW model complex was applied without further calibration (Bailey et al., 2016; Chunn et al., 2019), with calibration against only streamflow observations (Molina-Navarro et al., 2019), with separated calibration for streamflow and groundwater head (Guzman et al., 2015), or with simple manual calibration by graphically comparing the simulated and observed streamflow and groundwater head (Sith et al., 2019). Since both the SWAT and MODFLOW supporting software can use the inverse modeling (IM) method for calibration, and parameter non-uniqueness is an inherent property of IM (Abbaspour, 2015), the coupling of a calibrated SWAT and a calibrated MODFLOW cannot guarantee a proper or sufficiently optimized parameter set for the integrated SWAT-MODFLOW model. Because groundwater and surface water interact with each other, calibrating the simulation of one part does not guarantee proper simulation of the other part. Application of a combined calibration approach based on PEST allowed us to calibrate the SWAT-MODFLOW model by adjusting simultaneously SWAT and MODFLOW parameters and using observations of both streamflow and groundwater table when deriving the objective function. The calibration results demonstrated that the summary statistics of the SWAT-MODFLOW performance were improved by this approach (Table 6).



664 The ability of SWAT-MODFLOW to evaluate the impacts of groundwater abstraction on streamflow
 665 or groundwater-surface water interactions has been tested in the previous studies (Guzman et al., 2015;
 666 Chunn et al., 2019; Molina-Navarro et al., 2019). (Molina-Navarro et al., 2019), for example, also
 667 found that the SWAT model showed almost no impact of groundwater abstraction on streamflow
 668 depletion. Besides due to the simple representation of groundwater dynamics, the other cause of this,
 669 we believe, is that same as suggested above, that the impact of groundwater water removal by
 670 abstractions on water table fluctuations is currently not accounted for in the groundwater discharge
 671 calculation in the SWAT source code. Our findings are generally consistent with those of these
 672 previous studies, although all of the studies tested the effects of groundwater abstraction only by
 673 drinking water without considering irrigation and based on assumed drinking water pumping wells. In
 674 addition, in all the previous SWAT-MODFLOW studies, the River Package in the MODFLOW model
 675 was the only package used for simulating groundwater-surface water interaction, ignoring the potential
 676 drain flow processes. The SWAT-MODFLOW complex used in our study was further developed to
 677 allow application of the Drain Package and to allow also an auto-irrigation routine to extract water
 678 from groundwater grid cells; in this way the impacts of groundwater abstraction for both drinking
 679 water and irrigation could be assessed.

680 **4.4 Limitations and future research**

681 Several limitations to this study need to be acknowledged. The simulated head generated by the steady-
 682 state model was used as the initial head conditions for the transient model, as also suggested in other
 683 studies (Anderson et al., 2015; Doherty et al., 2010). The ideal simulated initial heads should be
 684 calibrated with the observed initial heads. However, we did not have enough observed heads at the
 685 beginning of the simulation period (1997), so we used the observed heads covering the period 1996-
 686 2010 for calibrating the original steady-state MODFLOW-NWT to obtain the simulated initial heads.
 687 Fortunately, the groundwater heads of the study area did not change much during the study period (Fig.
 688 9, Fig. 10) and the difference inherently exists between the observed and simulated heads, indicating
 689 that the error between the ideal simulated initial heads and the actually used simulated initial heads
 690 was small.

691 An approach based on PEST was utilized to calibrate streamflow and groundwater table variation
 692 simultaneously in our SWAT-MODFLOW simulation, which improved the model performance and
 693 enabled parameter sensitivity analysis for the model. However, only two wells with relatively
 694 continuous time series of observed groundwater head were available and used to calibrate the
 695 groundwater variation. Ideally, calibration would involve more wells with continuous time series of



696 observed head, but this limitation is anticipated to be minor in our study as the groundwater head did
697 not change much in our simulations and the change mainly followed the variation of recharge with
698 precipitation as its source.

699 The average annual streamflow difference and the regular pattern of daily streamflow difference
700 between the abstraction scenarios and the no-wells scenario were generally explained well, but,
701 surprisingly and unexpectedly, the streamflow difference between the scenario with only drinking
702 water wells and the no-wells scenario on 24 March, 2010, simulated by SWAT-MODFLOW at two
703 stations, were positive, being 1.54 and 0.55 m³ s⁻¹, respectively (Fig. 12). The streamflow difference
704 between the scenario with only irrigation wells and the no-wells scenario at station B on the extreme
705 peak flow day (16 October, 2014) simulated by SWAT was -5.2 m³ s⁻¹ but then became positive next
706 day, which cannot be explained well to our best of knowledge so far. However, we found that the
707 general results of this study were not influenced when modifying the value of these two unexpected
708 points to be expected.

709 Both the SWAT and SWAT-MODFLOW simulations were based on the “best” parameter combination
710 achieved through calibration, which was deemed to be satisfactory for the purpose of this study.
711 However, complex models such as SWAT and SWAT-MODFLOW are subject to non-uniqueness (i.e.
712 more than one parameter combination may yield satisfactory results), so future studies may need to
713 consider the uncertainty due to, for example, parameter uncertainty. The calibration tool SWAT-CUP
714 has already been able to evaluate SWAT parameter uncertainty, whereas the new approach based on
715 PEST to calibrate SWAT-MODFLOW needs to be further explored to adapt for model uncertainty
716 analysis.

717 Our results support our original hypothesis that SWAT-MODFLOW can produce more reliable results
718 in the simulation of the effects of groundwater abstraction for either drinking water or irrigation on
719 streamflow patterns. In addition, SWAT-MODFLOW can produce more outputs than SWAT.
720 However, SWAT-MODFLOW also requires more effort and data to be set up and calibrated, and
721 longer time to run (around 6 hours for a 19-year simulation in SWAT-MODFLOW by a desktop with
722 an Intel® Core™ Processor i7-6700 CPU and 16 GB installed RAM versus 6 minutes for a SWAT
723 simulation). Therefore, the balance between scientific accuracy and the computational burden should
724 be defined relative to the study goal when choosing between SWAT and SWAT-MODFLOW in a
725 future study. But clearly, if the purpose of a study is to investigate effects of groundwater abstraction
726 on streams, the efforts should be focused on setting up and applying a fully-distributed model in
727 groundwater domain, such as SWAT-MODFLOW. A graphical user interface has also been developed



728 to couple SWAT and MODFLOW based on the publically available version of the SWAT-
729 MODFLOW complex (Park et al., 2018). Since the SWAT-MODFLOW complex used in this study
730 was newly developed and allowed use of the Drain Package and auto-irrigation, a new graphical user
731 interface based on the new SWAT-MODFLOW complex could ensure that a study such as that
732 presented here is repeated with less effort and technical challenges.

733 5. Conclusions

734 SWAT and SWAT-MODFLOW models with relatively complex set-ups were applied to a lowland
735 catchment, the Uggerby River Catchment in Northern Denmark. Model performance and the outcome
736 of four groundwater abstraction scenarios (with real wells and abstraction rates) were analyzed and
737 compared.

738 Generally both models simulated well the temporal patterns of streamflow at the two hydrological
739 stations during the calibration and validation periods. SWAT-MODFLOW, however, showed superior
740 performance when visualizing time series results and when comparing summary statistics.
741 Furthermore, SWAT-MODFLOW generates many additional outputs for groundwater analysis, such
742 as spatial-temporal patterns of water table elevation and groundwater-surface water exchange rates at
743 cell or subbasin level, improving water resources management in a groundwater-dominated catchment.

744 Abstraction scenarios simulated by SWAT and SWAT-MODFLOW showed different signals in
745 streamflow change. The simulations by both models indicated that drinking water abstraction caused
746 streamflow depletion and that irrigation abstraction caused a slight total flow increase (but decreased
747 the soil or aquifer water storage, which may influence the hydrology outside the catchment). However,
748 the impact of drinking water abstraction on streamflow depletion by SWAT was minimal and
749 underestimated, and the streamflow increase caused by irrigation abstraction was exaggerated
750 compared with the SWAT-MODFLOW simulation, which produced more realistic results.

751 Overall, the new SWAT-MODFLOW model calibrated by PEST, which included the Drain Package
752 and a new auto-irrigation routine, presented a better hydrological simulation, wider possibilities for
753 groundwater analysis, and more realistic assessments of the impact of groundwater abstractions (for
754 either irrigation or drinking water purposes) on streamflow compared with SWAT. Thus, SWAT-
755 MODFLOW can be used as a tool for managing water resources in groundwater-affected catchments,
756 taking into account its higher computational demand and more time consumption.



757 *Code and data availability.*

758 The land use map based on the Danish Area Information System is freely available from
759 (https://www.dmu.dk/1_viden/2_miljoe-tilstand/3_samfund/ais/3_Metadata/metadaten.htm).

760 Climate data is available from the Danish Meteorological Institute (<https://www.dmi.dk/>). QGIS is
761 freely available from <https://qgis.org/en/site/>. QSWAT, SWATCUP, and the SWAT-MODFLOW as
762 well as its source codes are publicly available from <https://swat.tamu.edu/software>. The steady-state
763 MODFLOW set-up was provided by NIRAS upon request. The PEST utilities and tutorial are freely
764 downloadable from <http://www.pesthomepage.org/Home.php>. The source code, executable, and tutorial
765 for the further developed SWAT-MODFLOW are available on the SWAT website
766 (<https://swat.tamu.edu/software/swat-modflow/>). The two code files used for SWAT-MODFLOW
767 calibration by PEST will be available through repository on <https://www.re3data.org/> when the paper
768 is accepted.

769

770 *Author contributions.* DT and WL designed the study. WL undertook all practical elements of the
771 study, including setting up and calibrating the models, analyzing results, producing figures, and writing
772 the manuscript. SP and RTB contributed the idea and developed the codes for use of the PEST
773 approach to calibrate the SWAT-MODFLOW model. RTB provided the knowledge to set up SWAT-
774 MODFLOW and further developed the SWAT-MODFLOW complex codes. DT, EMN, HEA, HT,
775 and AN provided most of the data and contributed with their knowledge to setting up and calibrating
776 the models. DT and EJ helped to analyze the results and contributed to the discussion. JSJ and JBJ
777 provided the original steady-state MODFLOW-NWT set-up and contributed with relative knowledge.
778 All co-authors contributed to the manuscript writing.

779

780 *Competing interests.* The authors declare that they have no conflict of interest.

781

782 *Acknowledgements.*

783 The first author was supported by grants from the China Scholarship Council. Erik Jeppesen and
784 Dennis Trolle were supported by the AU Centre for Water Technology (WATEC). We thank Chenda
785 Deng, Xiaolu Wei, and Zaichen Xiang for technique assistance and knowledge exchange during Wei
786 Liu's research stay at the Colorado State University. We also thank Anne Mette Poulsen for valuable
787 editorial comments.

788

789

790



References

- Abbas, S., Xuan, Y., and Bailey, R.: Improving River Flow Simulation Using a Coupled Surface-Groundwater Model for Integrated Water Resources Management, 2018.
- Abbaspour, K. C.: SWAT-CUP: SWAT Calibration and Uncertainty Programs - A User Manual., 2015.
- Ali, R., McFarlane, D., Varma, S., Dawes, W., Emelyanova, I., Hodgson, G., and Charles, S.: Potential climate change impacts on groundwater resources of south-western Australia, *Journal of Hydrology*, 475, 456-472, <https://doi.org/10.1016/j.jhydrol.2012.04.043>, 2012.
- Aliyari, F., Bailey, R. T., Tasdighi, A., Dozier, A., Arabi, M., and Zeiler, K.: Coupled SWAT-MODFLOW model for large-scale mixed agro-urban river basins, *Environmental Modelling & Software*, 115, 200-210, <https://doi.org/10.1016/j.envsoft.2019.02.014>, 2019.
- Anderson, M. P., Woessner, W. W., and Hunt, R. J.: Chapter 7 - Steady-State and Transient Simulations, in: *Applied Groundwater Modeling (Second Edition)*, edited by: Anderson, M. P., Woessner, W. W., and Hunt, R. J., Academic Press, San Diego, 303-327, 2015.
- Aslyng, H.: Forelæsninger over vanding i jordbruget, DSR Forlag. Den kgl. Veterinær-og Landbohøjskole, 1983.
- Bailey, R., Rathjens, H., Bieger, K., Chaubey, I., and Arnold, J.: Swatmod-Prep: Graphical User Interface for Preparing Coupled Swat-Modflow Simulations, *J Am Water Resour As*, 53, 400-410, 10.1111/1752-1688.12502, 2017.
- Bailey, R. T., Wible, T. C., Arabi, M., Records, R. M., and Ditty, J.: Assessing regional-scale spatio-temporal patterns of groundwater-surface water interactions using a coupled SWAT-MODFLOW model, *Hydrological Processes*, 30, 4420-4433, 10.1002/hyp.10933, 2016.
- Cheema, M. J., Immerzeel, W. W., and Bastiaanssen, W. G.: Spatial quantification of groundwater abstraction in the irrigated Indus basin, *Ground Water*, 52, 25-36, 10.1111/gwat.12027, 2014.
- Chen, X. H., and Yin, Y. F.: Streamflow depletion: Modeling of reduced baseflow and induced stream infiltration from seasonally pumped wells, *J Am Water Resour As*, 37, 185-195, DOI 10.1111/j.1752-1688.2001.tb05485.x, 2001.
- Chen, Y., Marek, G., Marek, T., Brauer, D., and Srinivasan, R.: Assessing the Efficacy of the SWAT Auto-Irrigation Function to Simulate Irrigation, Evapotranspiration, and Crop Response to Management Strategies of the Texas High Plains, *Water-Sui*, 9, 10.3390/w9070509, 2017.
- Chunn, D., Faramarzi, M., Smerdon, B., and Alessi, D.: Application of an Integrated SWAT-MODFLOW Model to Evaluate Potential Impacts of Climate Change and Water Withdrawals on Groundwater-Surface Water Interactions in West-Central Alberta, *Water-Sui*, 11, 10.3390/w11010110, 2019.
- Doherty, J.: PEST: Model-independent parameter estimation and Uncertainty Analysis, User manual: [EB/OL], Brisbane, Queensland, Australia: Watermark Numeric Computing, 2018.
- Doherty, J. E., Hunt, R. J., and Tonkin, M. J.: Approaches to highly parameterized inversion: A guide to using PEST for model-parameter and predictive-uncertainty analysis, *US Geological Survey Scientific Investigations Report*, 5211, 71, 2010.
- Fukunaga, D. C., Cecilio, R. A., Zanetti, S. S., Oliveira, L. T., and Caiado, M. A. C.: Application of the SWAT hydrologic model to a tropical watershed at Brazil, *Catena*, 125, 206-213, 10.1016/j.catena.2014.10.032, 2015.
- Gao, F., Feng, G., Han, M., Dash, P., Jenkins, J., and Liu, C.: Assessment of Surface Water Resources in the Big Sunflower River Watershed Using Coupled SWAT-MODFLOW Model, *Water-Sui*, 11, 528, 2019.
- Gassman, P. W., Sadeghi, A. M., and Srinivasan, R.: Applications of the SWAT Model Special Section: Overview and Insights, *J Environ Qual*, 43, 1-8, 10.2134/jeq2013.11.0466, 2014.
- George, Y. D. R. S. C.: QGIS Interface for SWAT (QSWAT), 2017.
- GEUS: Water supply in Denmark, Danish Ministry of the Environment, Denmark, 18, 2009.
- Glover, R. E., and Balmer, G. G.: River depletion resulting from pumping a well near a river, *Eos, Transactions American Geophysical Union*, 35, 468-470, 1954.
- Greve, M. H., Greve, M. B., Bøcher, P. K., Balstrøm, T., Breuning-Madsen, H., and Krogh, L.: Generating a Danish raster-based topsoil property map combining choropleth maps and point information, *Geografisk Tidsskrift-Danish Journal of Geography*, 107, 1-12, 10.1080/00167223.2007.10649565, 2007.



- 842 Güngör, Ö., and Göncü, S.: Application of the soil and water assessment tool model on the Lower Porsuk
 843 Stream Watershed, *Hydrological Processes*, 27, 453-466, 10.1002/hyp.9228, 2013.
- 844 Guzman, J. A., Moriasi, D. N., Gowda, P. H., Steiner, J. L., Starks, P. J., Arnold, J. G., and Srinivasan, R.: A model
 845 integration framework for linking SWAT and MODFLOW, *Environmental Modelling & Software*, 73, 103-116,
 846 10.1016/j.envsoft.2015.08.011, 2015.
- 847 Henriksen, H. J., Trolborg, L., Højberg, A. L., and Refsgaard, J. C.: Assessment of exploitable groundwater
 848 resources of Denmark by use of ensemble resource indicators and a numerical groundwater-surface water
 849 model, *Journal of Hydrology*, 348, 224-240, 10.1016/j.jhydrol.2007.09.056, 2008.
- 850 Huang, C.-S., Yang, T., and Yeh, H.-D.: Review of analytical models to stream depletion induced by pumping:
 851 Guide to model selection, *Journal of Hydrology*, 561, 277-285, <https://doi.org/10.1016/j.jhydrol.2018.04.015>,
 852 2018.
- 853 Hunt, B.: Unsteady stream depletion from ground water pumping, *Groundwater*, 37, 98-102, 1999.
- 854 Izady, A., Davary, K., Alizadeh, A., Ziaei, A. N., Akhavan, S., Alipoor, A., Joodavi, A., and Brusseau, M. L.:
 855 Groundwater conceptualization and modeling using distributed SWAT-based recharge for the semi-arid
 856 agricultural Neishaboor plain, Iran, *Hydrogeol J*, 23, 47-68, 10.1007/s10040-014-1219-9, 2015.
- 857 Jeppesen, E., Brucet, S., Naselli-Flores, L., Papastergiadou, E., Stefanidis, K., Nöges, T., Nöges, P., Attayde, J. L.,
 858 Zohary, T., Coppens, J., Bucak, T., Menezes, R. F., Freitas, F. R. S., Kernan, M., Søndergaard, M., and Beklioglu,
 859 M.: Ecological impacts of global warming and water abstraction on lakes and reservoirs due to changes in
 860 water level and related changes in salinity, *Hydrobiologia*, 750, 201-227, 10.1007/s10750-014-2169-x, 2015.
- 861 Johansen, O. M., Pedersen, M. L., and Jensen, J. B.: Effect of groundwater abstraction on fen ecosystems,
 862 *Journal of Hydrology*, 402, 357-366, 10.1016/j.jhydrol.2011.03.031, 2011.
- 863 Kim, N. W., Chung, I. M., Won, Y. S., and Arnold, J. G.: Development and application of the integrated SWAT-
 864 MODFLOW model, *Journal of Hydrology*, 356, 1-16, 10.1016/j.jhydrol.2008.02.024, 2008.
- 865 Knudsen, T., and Olsen, B. P.: Proceedings of the 2nd NKG workshop on national DEMs, Technical report No.4,
 866 National Survey and Cadastre, Danish Ministry of the Environment, Copenhagen, Denmark, 36, 2008.
- 867 Lachal, F., Mlayah, A., Bédir, M., Tarhouni, J., and Leduc, C.: Implementation of a 3-D groundwater flow model
 868 in a semi-arid region using MODFLOW and GIS tools: The Zéramdine-Béni Hassen Miocene aquifer system
 869 (east-central Tunisia), *Computers & Geosciences*, 48, 187-198, 10.1016/j.cageo.2012.05.007, 2012.
- 870 Lee, K.-S., Chung, E.-S., and Shin, M.-J.: Effects of changes of climate, groundwater withdrawal, and landuse
 871 on total flow during dry period, *Journal of Korea Water Resources Association*, 39, 923-934, 2006.
- 872 Liu, W., An, W., Jeppesen, E., Ma, J., Yang, M., and Trolle, D.: Modelling the fate and transport of
 873 *Cryptosporidium*, a zoonotic and waterborne pathogen, in the Daning River watershed of the Three Gorges
 874 Reservoir Region, China, *J Environ Manage*, 232, 462-474, <https://doi.org/10.1016/j.jenvman.2018.10.064>,
 875 2019.
- 876 Lu, S., Kronvang, B., Audet, J., Trolle, D., Andersen, H. E., Thodsen, H., and van Griensven, A.: Modelling
 877 sediment and total phosphorus export from a lowland catchment: Comparing sediment routing methods,
 878 *Hydrological processes*, 29, 280-294, 2015.
- 879 Lu, S., Andersen, H. E., Thodsen, H., Rubæk, G. H., and Trolle, D.: Extended SWAT model for dissolved reactive
 880 phosphorus transport in tile-drained fields and catchments, *Agricultural Water Management*, 175, 78-90,
 881 10.1016/j.agwat.2015.12.008, 2016.
- 882 Malago, A., Bouraoui, F., Vigiak, O., Grizzetti, B., and Pastori, M.: Modelling water and nutrient fluxes in the
 883 Danube River Basin with SWAT, *Sci Total Environ*, 603-604, 196-218, 10.1016/j.scitotenv.2017.05.242, 2017.
- 884 Markstrom, S. L., Niswonger, R. G., Regan, R. S., Prudic, D. E., and Barlow, P. M.: GSFLOW-Coupled Ground-
 885 water and Surface-water FLOW model based on the integration of the Precipitation-Runoff Modeling System
 886 (PRMS) and the Modular Ground-Water Flow Model (MODFLOW-2005), *US Geological Survey techniques and
 887 methods*, 6, 240, 2008.
- 888 Markstrom, S. L., Regan, R. S., Hay, L. E., Viger, R. J., Webb, R. M., Payn, R. A., and LaFontaine, J. H.: PRMS-IV,
 889 the precipitation-runoff modeling system, version 4, *US Geological Survey Techniques and Methods*, 2015.
- 890 May, R., and Mazlan, N. S. B.: Numerical simulation of the effect of heavy groundwater abstraction on
 891 groundwater-surface water interaction in Langat Basin, Selangor, Malaysia, *Environmental Earth Sciences*, 71,
 892 1239-1248, 10.1007/s12665-013-2527-4, 2014.



- 893 Molina-Navarro, E., Andersen, H. E., Nielsen, A., Thodsen, H., and Trolle, D.: The impact of the objective
 894 function in multi-site and multi-variable calibration of the SWAT model, *Environmental Modelling & Software*,
 895 93, 255-267, 10.1016/j.envsoft.2017.03.018, 2017.
- 896 Molina-Navarro, E., Bailey, R. T., Andersen, H. E., Thodsen, H., Nielsen, A., Park, S., Jensen, J. S., Jensen, J. B.,
 897 and Trolle, D.: Comparison of abstraction scenarios simulated by SWAT and SWAT-MODFLOW, *Hydrological*
 898 *Sciences Journal*, 2019.
- 899 Moriasi, D. N., Gitau, M. W., Pai, N., and Daggupati, P.: Hydrologic and water quality models: Performance
 900 measures and evaluation criteria, *Transactions of the ASABE*, 58, 1763-1785, 2015.
- 901 NERI: Metadata for the area information system (in Danish: Metadata for Arealinformation Systemet). Danish
 902 National Environmental Research Institute, Roskilde, 2000.
- 903 Nguyen, V. T., and Dietrich, J.: Modification of the SWAT model to simulate regional groundwater flow using
 904 a multicell aquifer, *Hydrological Processes*, 32, 939-953, 10.1002/hyp.11466, 2018.
- 905 Nielsen, A., Trolle, D., Me, W., Luo, L., Han, B.-P., Liu, Z., Olesen, J. E., and Jeppesen, E.: Assessing ways to
 906 combat eutrophication in a Chinese drinking water reservoir using SWAT, *Marine and Freshwater Research*,
 907 64, 475, 10.1071/mf12106, 2013.
- 908 Niswonger, R. G., Panday, S., and Ibaraki, M.: MODFLOW-NWT, a Newton formulation for MODFLOW-2005,
 909 *US Geological Survey Techniques and Methods*, 6, 44, 2011.
- 910 Pardo, I., and Garcia, L.: Water abstraction in small lowland streams: Unforeseen hypoxia and anoxia effects,
 911 *Science of the Total Environment*, 568, 226-235, 10.1016/j.scitotenv.2016.05.218, 2016.
- 912 Park, S.: Enhancement of Coupled Surface/Subsurface Flow Models in Watersheds: Analysis, Model
 913 Development, Optimization, and User Accessibility, Colorado State University, 2018.
- 914 Park, S., Nielsen, A., Bailey, R. T., Trolle, D., and Bieger, K.: A QGIS-based graphical user interface for application
 915 and evaluation of SWAT-MODFLOW models, *Environmental Modelling & Software*,
 916 <https://doi.org/10.1016/j.envsoft.2018.10.017>, 2018.
- 917 Parkin, G., Birkinshaw, S. J., Younger, P. L., Rao, Z., and Kirk, S.: A numerical modelling and neural network
 918 approach to estimate the impact of groundwater abstractions on river flows, *Journal of Hydrology*, 339, 15-
 919 28, 10.1016/j.jhydrol.2007.01.041, 2007.
- 920 Pfannerstill, M., Guse, B., and Fohrer, N.: A multi-storage groundwater concept for the SWAT model to
 921 emphasize nonlinear groundwater dynamics in lowland catchments, *Hydrological Processes*, 28, 5573-5612,
 922 10.1002/hyp.10062, 2014.
- 923 Poulsen, J. B.: Stream flow-its estimation, uncertainty and interaction with groundwater and floodplains,
 924 Aarhus University, 2013.
- 925 Sanz, D., Castano, S., Cassiraga, E., Sahuquillo, A., Gomez-Alday, J. J., Pena, S., and Calera, A.: Modeling aquifer-
 926 river interactions under the influence of groundwater abstraction in the Mancha Oriental System (SE Spain),
 927 *Hydrogeol J*, 19, 475-487, 10.1007/s10040-010-0694-x, 2011.
- 928 Semiromi, M. T., and Koch, M.: Analysis of spatio-temporal variability of surface-groundwater interactions in
 929 the Gharehsoo river basin, Iran, using a coupled SWAT-MODFLOW model, *Environmental Earth Sciences*, 78,
 930 201, 2019.
- 931 Shafeeqe, M., Cheema, M. J. M., Sarwar, A., and Hussain, M. W.: Quantification of Groundwater Abstraction
 932 Using Swat Model in Hakra Branch Canal System of Pakistan, *Pak J Agr Sci*, 53, 249-255, Doi
 933 10.21162/Pakjas/16.4199, 2016.
- 934 Sith, R., Watanabe, A., Nakamura, T., Yamamoto, T., and Nadaoka, K.: Assessment of water quality and
 935 evaluation of best management practices in a small agricultural watershed adjacent to Coral Reef area in Japan,
 936 *Agricultural Water Management*, 213, 659-673, <https://doi.org/10.1016/j.agwat.2018.11.014>, 2019.
- 937 Stefania, G. A., Rotiroti, M., Fumagalli, L., Simonetto, F., Capodaglio, P., Zanotti, C., and Bonomi, T.: Modeling
 938 groundwater/surface-water interactions in an Alpine valley (the Aosta Plain, NW Italy): the effect of
 939 groundwater abstraction on surface-water resources, *Hydrogeol J*, 26, 147-162, 10.1007/s10040-017-1633-x,
 940 2018.
- 941 Surinaidu, L., Gurunadha Rao, V. V. S., Srinivasa Rao, N., and Srinu, S.: Hydrogeological and groundwater
 942 modeling studies to estimate the groundwater inflows into the coal Mines at different mine development



943 stages using MODFLOW, Andhra Pradesh, India, Water Resources and Industry, 7-8, 49-65,
 944 10.1016/j.wri.2014.10.002, 2014.
 945 Thodsen, H., Andersen, H. E., Blicher-Mathiesen, G., and Trolle, D.: The combined effects of fertilizer reduction
 946 on high risk areas and increased fertilization on low risk areas, investigated using the SWAT model for a Danish
 947 catchment, *Acta Agriculturae Scandinavica, Section B — Soil & Plant Science*, 65, 217-227,
 948 10.1080/09064710.2015.1010564, 2015.
 949 Vainu, M., and Terasmaa, J.: The consequences of increased groundwater abstraction for groundwater
 950 dependent closed-basin lakes in glacial terrain, *Environmental Earth Sciences*, 75, ARTN 9210.1007/s12665-
 951 015-4967-5, 2016.
 952 Wei, X., Bailey, R. T., Records, R. M., Wible, T. C., and Arabi, M.: Comprehensive simulation of nitrate transport
 953 in coupled surface-subsurface hydrologic systems using the linked SWAT-MODFLOW-RT3D model,
 954 *Environmental Modelling & Software*, 10.1016/j.envsoft.2018.06.012, 2018.
 955 Yi, L., and Sophocleous, M.: Two-way coupling of unsaturated-saturated flow by integrating the SWAT and
 956 MODFLOW models with application in an irrigation district in arid region of West China, *J Arid Land*, 3, 164-
 957 173, 2011.
 958 Zhang, X., Ren, L., and Kong, X.: Estimating spatiotemporal variability and sustainability of shallow
 959 groundwater in a well-irrigated plain of the Haihe River basin using SWAT model, *Journal of Hydrology*, 541,
 960 1221-1240, 10.1016/j.jhydrol.2016.08.030, 2016.
 961 Zhulu, L.: *Getting Started with PEST*, Athens, The University of Georgia, 2010.
 962 Zipper, S. C., Gleeson, T., Kerr, B., Howard, J. K., Rohde, M. M., Carah, J., and Zimmerman, J.: Rapid and accurate
 963 estimates of streamflow depletion caused by groundwater pumping using analytical depletion functions, 2018.

964
 965
 966
 967
 968
 969
 970
 971
 972
 973
 974
 975
 976
 977
 978
 979
 980
 981
 982
 983
 984
 985
 986
 987
 988
 989
 990
 991
 992
 993



Table 1. Farm types and crop rotations used to describe agricultural management in the Uggerby
 River Catchment (W: winter, S: spring).

Rotation type	Farm Type	Manure N (kg N/ha)	% Farm area	Rotation scheme				
				Year 1	Year 2	Year 3	Year 4	Year 5
Agricultural land 1	Mixed and horticulture	<50	31.0	W. wheat	W. wheat	S. barley	W. rape	S. barley
Agricultural land 2	Dairy/Cattle	85-170	35.7	S. barley	Grass	S. barley	Grass	Grass
Agricultural land 3	Dairy/Cattle	85-170	33.3	S. barley	S. barley	W. wheat	Corn silage	Corn silage



Table 2. Initial ranges and calibrated values of the selected parameters for SWAT calibration.

Parameter	Description	Initial range	Calibrated values	
			Subbasins: 4,5,7-13 (upstream)	Subbasins: 1,3,6,14-19 (downstream)
v__SFTMP.bsn	Snowfall temperature (°C)	-1 – 1	0.175	
v__SMFMN.bsn	Melt factor for snow on December 21 (mm H ₂ O °C ⁻¹ d ⁻¹)	1 – 2	1.287	
v__SMFMX.bsn	Melt factor for snow on June 21 (mm H ₂ O °C ⁻¹ d ⁻¹)	1.6 – 3.5	2.467	
v__SMTMP.bsn	Snow melt base temperature (°C)	-2.3 – 1	-1.342	
v__SURLAG.bsn	Surface runoff lag coefficient	1 – 10	6.379	
v__ALPHA_BF.gw	Baseflow alpha factor for shallow aquifer (l d ⁻¹)	0 – 1	0.453	0.639
v__ALPHA_BF_D.gw	Baseflow alpha factor for deep aquifer (l d ⁻¹)	0 – 1	0.756	0.913
v__ALPHA_BNK.rte	Baseflow alpha factor for bank storage (l d ⁻¹)	0 – 1	0.912	0.533
v__CH_K2.rte	Effective hydraulic conductivity in main channel alluvium (mm h ⁻¹)	0 – 75	57.068	45.018
r__CN2.mgt	Initial SCS runoff curve number for moisture condition II	-0.3 – 0.3	-0.279	0.137
r__DDRAIN.mgt	Depth to subsurface drain (mm)	-0.3 – 0.3	0.066	-0.129
v__EPCO.hru	Plant uptake compensation factor	0.01 – 1	0.163	0.254
v__ESCO.hru	Soil evaporation compensation factor	0 – 1	0.466	0.931
r__GDRAIN.mgt	Drain tile lag time (h)	-0.3 – 0.3	0.052	-0.021
v__GWQMN.gw	Threshold depth of water in the shallow aquifer required for return flow to occur (mm)	0 – 2000	1435.04	960.32
v__GW_DELAY.gw	Groundwater delay time (d)	0 – 200	116.28	123.40
v__GW_REVAP.gw	Groundwater “revap” coefficient	0.02 – 0.1	0.092	0.0313
r__OV_N.hru	Manning’s “n” value for overland flow	-0.2 – 0.2	-0.037	-0.025
v__REVAPMN.gw	Threshold depth of water in the shallow aquifer for “revap” or percolation to the deep aquifer to occur (mm)	1000 – 2000	1633.81	1521.80
r__SOL_AWC().sol	Available water capacity of the soil layer (mm H ₂ O mm soil ⁻¹)	-0.8 – 0.8	-0.674	0.786
r__SOL_BD().sol	Moist bulk density (g cm ⁻³)	-0.2 – 0.2	-0.067	0.156
r__SOL_K().sol	Saturated hydraulic conductivity (mm h ⁻¹)	-0.8 – 2	1.290	1.831
r__TDRAIN.mgt	Time to drain soil to field capacity (h)	-0.3 – 0.3	-0.097	-0.210
v__RCHRG_DP.gw	Deep aquifer percolation fraction	0 – 0.4	0.296	0.219
AUTO_WSTRS	Water stress threshold that triggers irrigation (mm)	70	30, 40, 60	

Note: v_ means that the existing parameter value is to be replaced by a given value; r_ means that an existing parameter value is multiplied by (1+ a given value).



Table 3. Initial values, ranges, and calibrated values of the selected parameters for SWAT-MODFLOW calibration using PEST.

Parameter	Description	Initial value	Parameter ranges	Calibrated values
v__SFTMP.bsn	---	0.175	-0.946–0.351	0.351
v__SMFMN.bsn	---	1.287	1.117–1.424	1.424
v__SMFMX.bsn	---	2.467	2.387–3.129	2.387
v__SMTMP.bsn	---	-1.342	-1.687– -0.46	-0.46
v__SURLAG.bsn	---	6.379	4.452– 8.151	4.964
v__ALPHA_BNK.rte ^a	---	0.912	0.7– 1	0.7
v__ALPHA_BNK.rte ^b	---	0.533	0.206– 0.617	0.231
v__CH_K2.rte ^a	---	57.068	29.322– 59.779	59.779
v__CH_K2.rte ^b	---	45.018	30.246– 60.088	41.182
r__CN2.mgt ^a	---	-0.279	-0.3– -0.106	-0.3
r__CN2.mgt ^b	---	0.137	-0.019– 0.175	0.0004
v__EPCO.hru ^a	---	0.163	0.077– 0.436	0.436
v__EPCO.hru ^b	---	0.255	0.01– 0.334	0.304
v__ESCO.hru ^a	---	0.466	0.227– 0.681	0.227
v__ESCO.hru ^b	---	0.931	0.684– 1	0.943
r__OV_N.hru ^a	---	-0.037	-0.2– -0.02	-0.02
r__OV_N.hru ^b	---	-0.025	-0.155– -0.005	-0.023
r__SOL_AWC().sol ^a	---	-0.675	-0.8– -0.316	-0.508
r__SOL_AWC().sol ^b	---	0.786	0.344– 0.8	0.8
r__SOL_BD().sol ^a	---	-0.067	-0.187– -0.05	-0.185
r__SOL_BD().sol ^b	---	0.156	0.077– 0.2	0.172
r__SOL_K().sol ^a	---	1.29	0.902– 2	0.902
r__SOL_K().sol ^b	---	1.831	1.012– 2	1.012
COND_1	Drain conductance	0.00467	0.00311 – 0.00622	0.00543
COND_2	Drain conductance	0.02487	0.01658 – 0.03316	0.03316
HK_CLAY	Hydraulic conductivity of clay (m s ⁻¹)	3.84E-08	1E-09 – 4.4E-08	2.2E-08
HK_SILT	Hydraulic conductivity of silt (m s ⁻¹)	5.00E-07	1E-07 – 9E-07	1E-07
HK_SS	Hydraulic conductivity of silty sand (m s ⁻¹)	6.70E-06	1.51E-06 – 7.50E-06	7.5E-06
HK_SSCS	Hydraulic conductivity of silty sand and clean sand (m s ⁻¹)	1.79E-05	1E-05 – 8E-05	1.79E-05
HK_CS	Hydraulic conductivity of clean sand (m s ⁻¹)	0.000327	1E-04 – 5E-04	3.15E-04
SS_CLAY	Specific storage of clay (m ⁻¹)	0.001099	9.19E-04 – 1.28E-03	1.28E-03
SS_SILT	Specific storage of silt (m ⁻¹)	0.000755	4.92E-04 – 1.02E-03	1.02E-03
SS_SAND	Specific storage of sand (m ⁻¹)	0.000166	1.28E-04 – 2.03E-04	2.03E-04
SY_CLAY	Specific yield of clay (%)	0.06	0.04 – 0.08	0.04
SY_SILT	Specific yield of silt (%)	0.2	0.15 – 0.25	0.22
SY_SAND	Specific yield of sand (%)	0.32	0.25 – 0.35	0.35
AUTO_WSTRS	---	30, 40, 60	30, 40, 60, 80	

Notes: “a” means that the parameter applies to the upstream areas, including subbasins: 4, 5, 7-13, while “b” applies to downstream areas, including subbasins 1, 3, 6, 14-19. “---” indicates that the corresponding parameters can be found in Table 2.



Table 4. The summary statistics for the calibrated MODFLOW performance.

Layer number	The number of observed heads	M_E (Mean error)	M_{AE} (Mean absolute error)	R_{MSE} (Root mean squared error)
Layer 1	453	-0.59	1.94	2.84
Layer 3	572	-0.54	2.36	3.15
Layer 5	38	-1.24	3.44	5.00
All	1063	-0.59	2.22	3.11

1044

1045

1046

1047

1048

1049

1050

1051

1052

1053

1054

1055

1056

1057

1058

1059

1060

1061

1062

1063

1064

1065

1066

1067

1068

1069

1070

1071

1072

1073

1074

1075



Table 5. Performance statistics indices for daily runoff at the outlets of subbasin 13 and subbasin 18 during the calibration (2001-2008) and validation (2009-2015, in brackets) periods by SWAT, SWAT-MODFLOW without PEST calibration, and SWAT-MODFLOW with PEST calibration.

Outlets	Used models	P _{BIAS}	N _{SE}	R ²
Subbasin 13 outlet	SWAT	-3.9 (5.9)	0.66 (0.50)	0.67 (0.53)
	SWAT-MODFLOW without PEST calibration	-6.9 (1.7)	0.72 (0.51)	0.75 (0.60)
	SWAT-MODFLOW with PEST calibration	1.9 (9.4)	0.78 (0.54)	0.78 (0.61)
Subbasin 18 outlet	SWAT	2.0 (12.4)	0.74 (0.47)	0.74 (0.53)
	SWAT-MODFLOW without PEST calibration	1.0 (11.0)	0.77 (0.46)	0.79 (0.57)
	SWAT-MODFLOW with PEST calibration	3.3 (13.1)	0.81 (0.53)	0.82 (0.60)



Table 6. Summary statistics for the SWAT-MODFLOW calibration result.

Observation group	Number of observed data	Weight of observed data	Contribution to squared weighted residuals before calibration by PEST	Contribution to squared weighted residuals after calibration by PEST
Streamflow A	2557	2	4410.3	3479.7
Streamflow B	2557	1	4911.7	4025.3
Well A	570	1	113	154.9
Well B	961	1	946.6	908.6
Sum	6645	---	10381	8568.5



Table 7. Average annual summary of the main components in the hydrological cycle of the Uggerby River Catchment during the study period (2002-2015) simulated by SWAT and SWAT-MODFLOW, respectively.

Components	SWAT	SWAT-MODFLOW
Precipitation (mm yr ⁻¹)	923	923
Surface flow (mm yr ⁻¹)	22	30
Lateral subsurface flow (mm yr ⁻¹)	89	64
Tile drain flow (mm yr ⁻¹)	20	0
Drain (MODFLOW, mm yr ⁻¹)	0	268
Groundwater flow (mm yr ⁻¹)	257	22
Total water yield (mm yr ⁻¹)	388	384
Actual evapotranspiration (mm yr ⁻¹)	503	516
Potential evapotranspiration (mm yr ⁻¹)	727	726
Soil storage (mm yr ⁻¹)	32	22
Average annual irrigation amount in the irrigated HRUs (mm yr ⁻¹)	137	133



Table 8. Average annual stream flow change (2002-2015) at subbasin 13 outlet and subbasin 18 outlet for each abstraction scenario from no-wells scenario and the corresponding annual abstraction simulated in SWAT and SWAT-MODFLOW

Scenarios		Scenario 2 (Only drinking water wells)		Scenario 3 (Only irrigation wells)		Scenario 4 (Both drinking water and irrigation wells)	
		SWAT	SWAT-MODFLOW	SWAT	SWAT-MODFLOW	SWAT	SWAT-MODFLOW
Average annual stream flow decrease(-) or increase(+) ($10^6 \text{ m}^3 \text{ yr}^{-1}$)	Subbasin 13 outlet	-0.024	-1.10	0.61	0.24	0.59	-0.73
	Subbasin 18 outlet	-0.12	-2.53	1.60	-0.55	1.48	-1.79
	Subbasins 4-5, 7-13	1.10	1.28	17.86	19.45	18.96	20.73
Annual abstraction ($10^6 \text{ m}^3 \text{ yr}^{-1}$)	The entire catchment excluding subbasin 19	4.01	3.96	40.54	39.26	44.55	43.22

Notes: Subbasin 13 outlet receives streamflow from subbasins 4-5, 7-13; Subbasin 18 outlet receives streamflow from the entire catchment excluding subbasin 19.

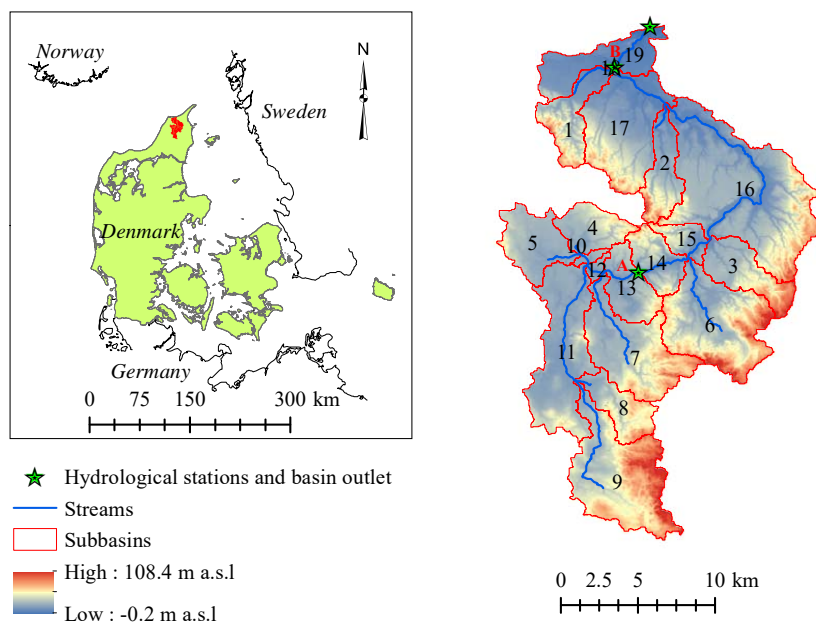


Figure 1. Location of the Uggerby catchment and its delineation in SWAT, including subbasins division, stream network definition based on the digital elevation model (DEM), hydrological monitoring stations, and basin outlet.

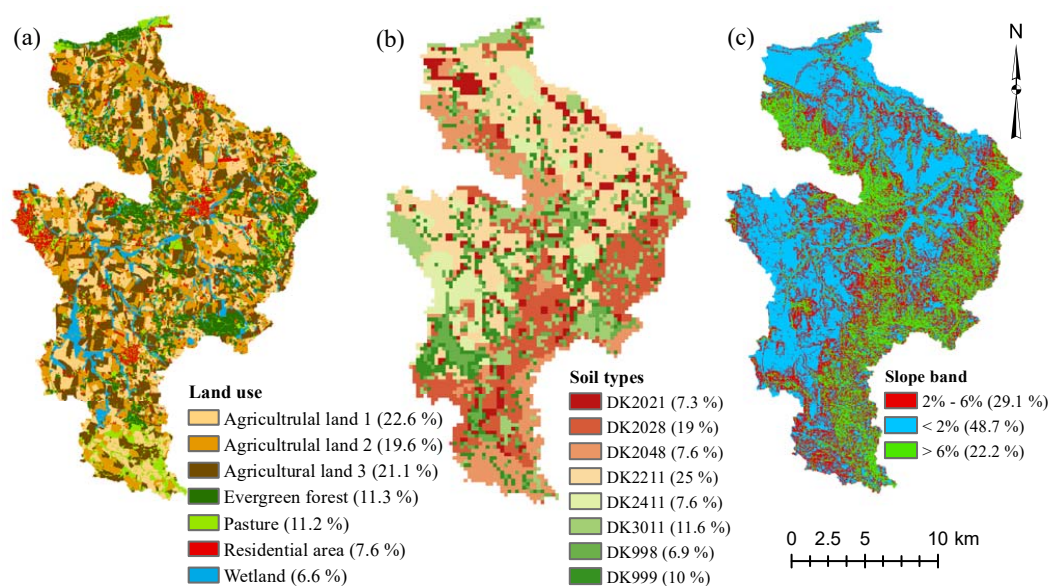


Figure 2. The distribution and proportion of each land use (a), soil type (b), and slope band (c) after reclassification for HRU definition in SWAT.

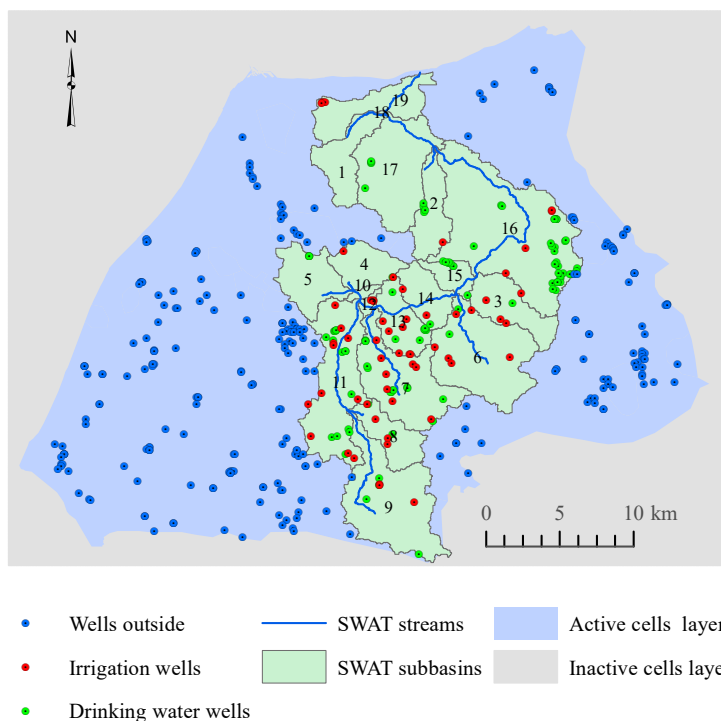


Figure 3. SWAT and MODFLOW set-up coverage and the well locations distributed inside or outside the Uggerby River Catchment.

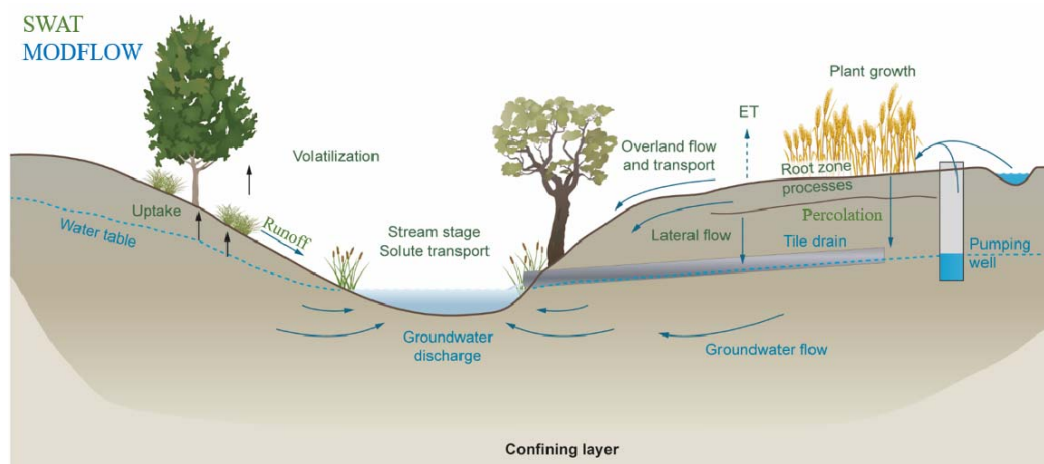


Figure 4. Schematic representation of water transport routes in stream-aquifer system as simulated by SWAT-MODFLOW, showing SWAT (green) and MODFLOW (blue) simulation processes. Adapted from (Molina-Navarro et al., 2019).

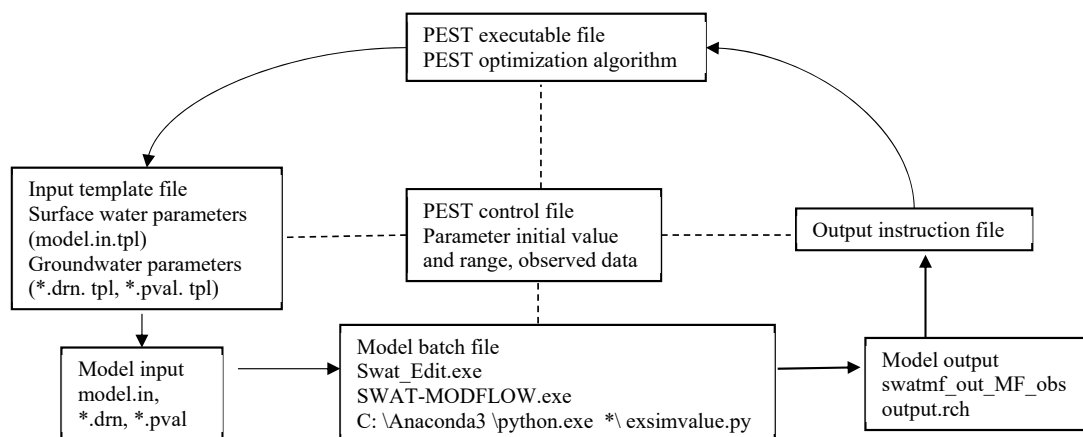


Figure 5. Schematic diagram of the PEST optimization process. The “*” means file name or file path.

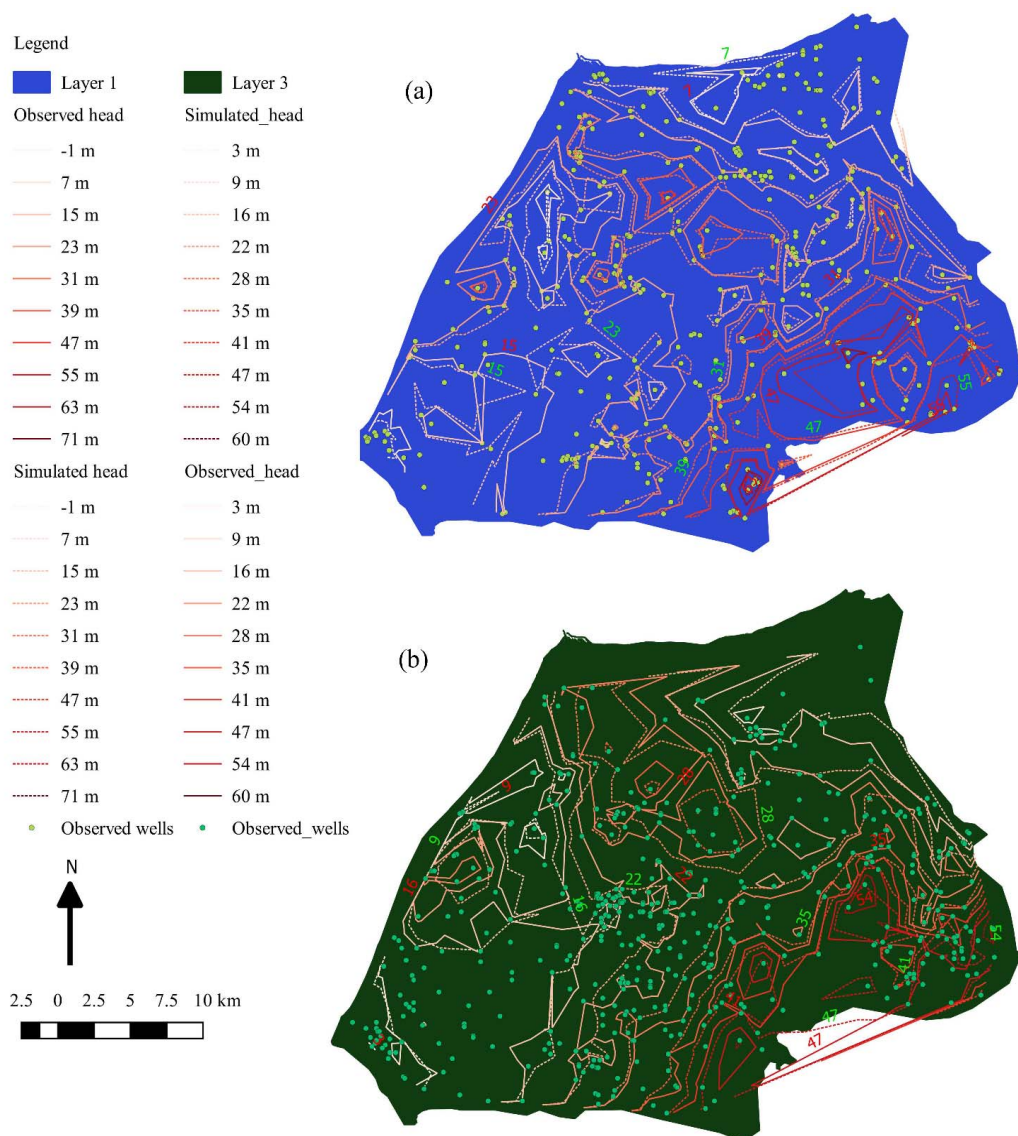


Figure 6. The simulated and observed head contours as well as the locations of observed wells within layer 1 (a) and layer 3 (b), respectively.

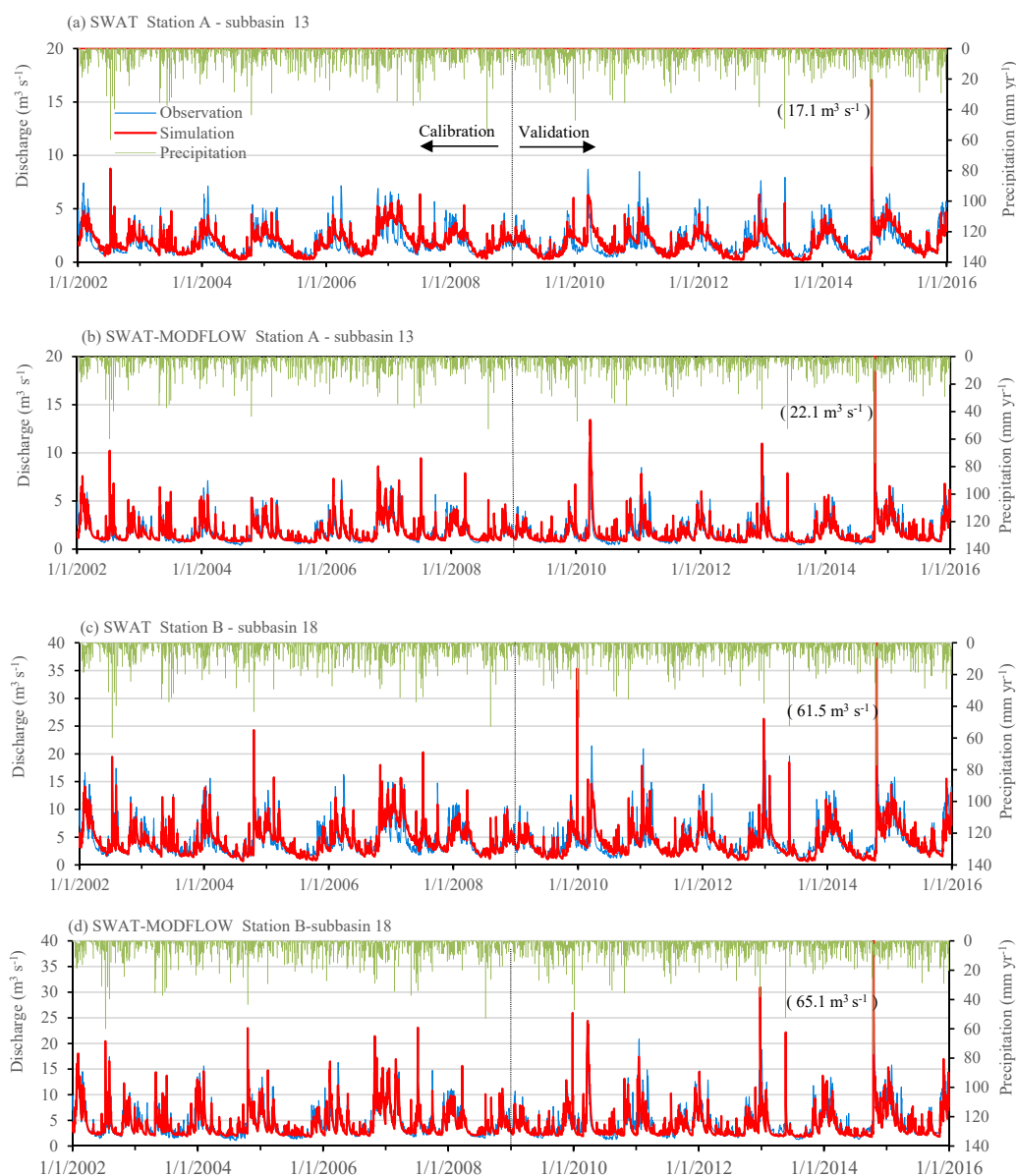


Figure 7. Hydrographs of precipitation, observed and best simulated daily streamflow at the outlets of subbasin 13 (station A) and subbasin 18 (station B) during the calibration period (2002–2008) and the validation period (2009–2015) based on SWAT and SWAT-MODFLOW. The value in bracket is the discharge on 16 October, 2014, which is outside the range of the plot area.

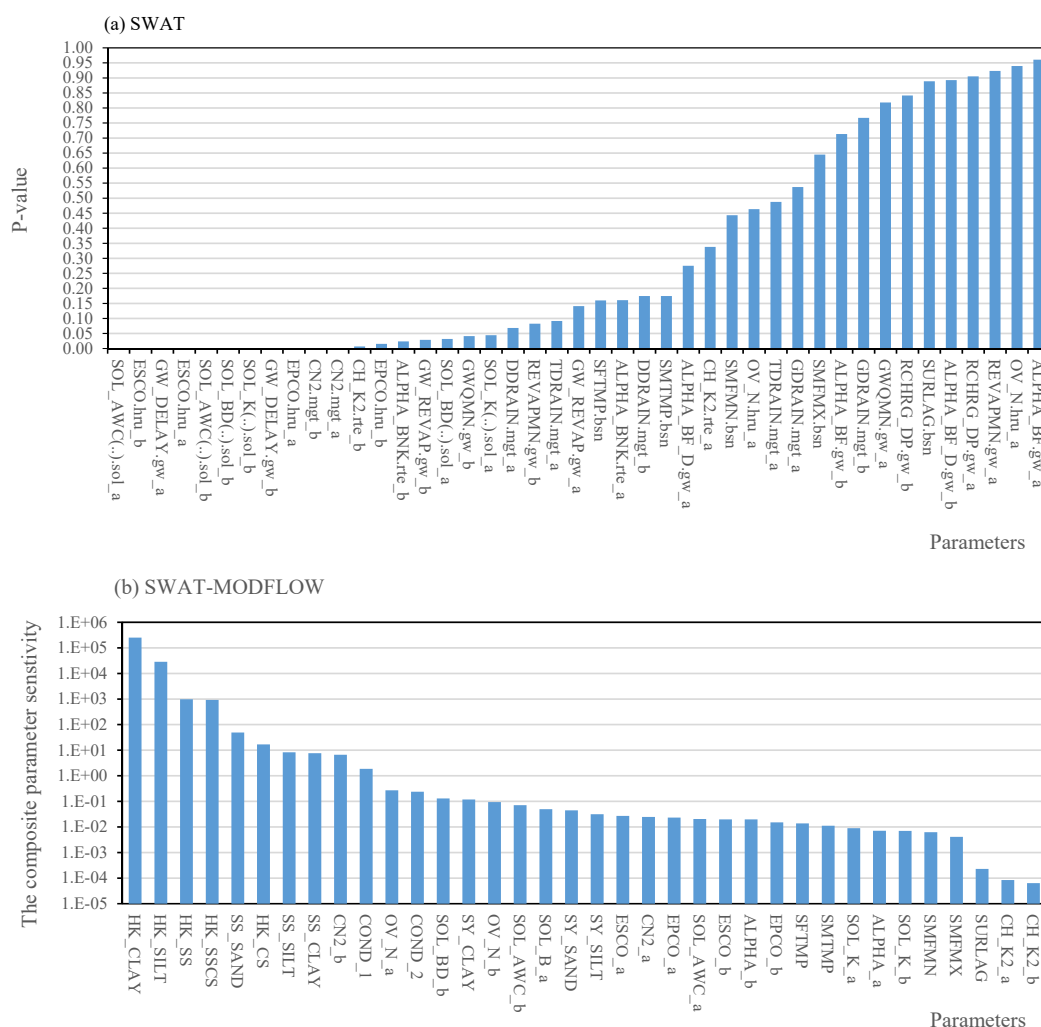


Figure 8. The sensitivity ranking of parameters in SWAT (a) and SWAT-MODFLOW (b) during calibration. The composite sensitivity of parameters was calculated based on the Jacobian matrix and the weight matrix after each PEST iteration and generated as an output once the PEST calibration was finished. The composite sensitivity values vary a little among the different iterations. The average value of each parameter among the 10 iterations for calibration is shown in the figure. More details regarding composite parameter sensitivity can be found in (Doherty, 2018). The “a” indicates that the parameter applies to the upstream areas, including subbasins: 4, 5, 7-13, and “b” indicates that the parameter applies to downstream areas, including subbasins 1, 3, 6, 14-19.

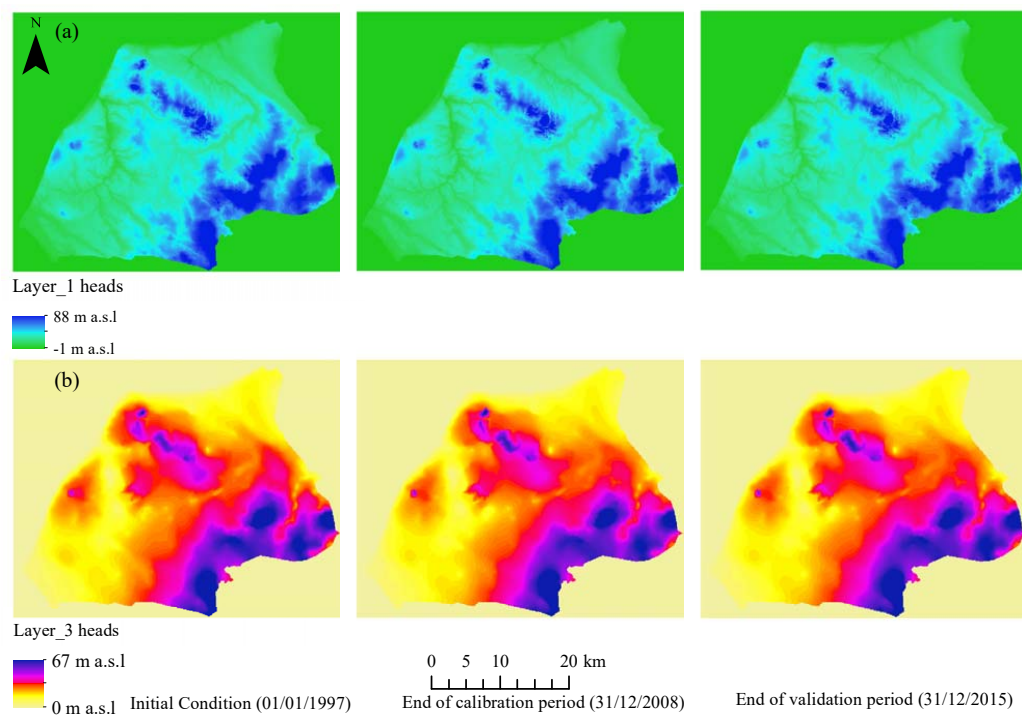


Figure 9. The simulated groundwater heads for the first layer (a) and third layer (b) at initial conditions, end of calibration period, and end of validation period by the calibrated SWAT-MODFLOW.

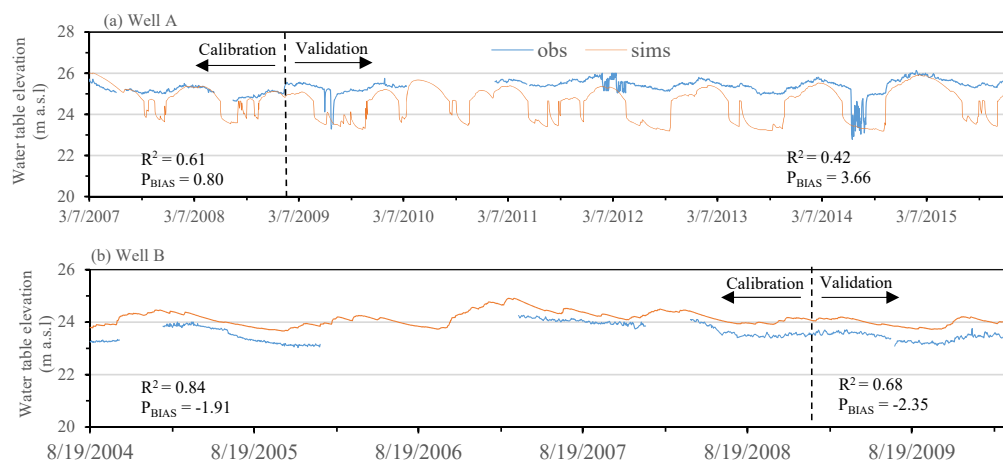


Figure 10. Hydrograph of daily simulated and observed groundwater heads (m a.s.l) of the two wells located in layer 1 used for calibrating the variation of groundwater heads simulated by SWAT-MODFLOW where relatively continuous observed data is available. Also shown are summary performance statistics.



Figure 11. Average annual water yield (total flow) (2002-2015) simulated for the scenarios (no wells, scenario 1; only drinking water wells, scenario 2; only irrigation wells, scenario 3; both drinking water and irrigation wells, scenario 4) with SWAT (a) and SWAT-MODFLOW (b) and divided into flow components (Q = flow; GW = groundwater; AQ = aquifer).

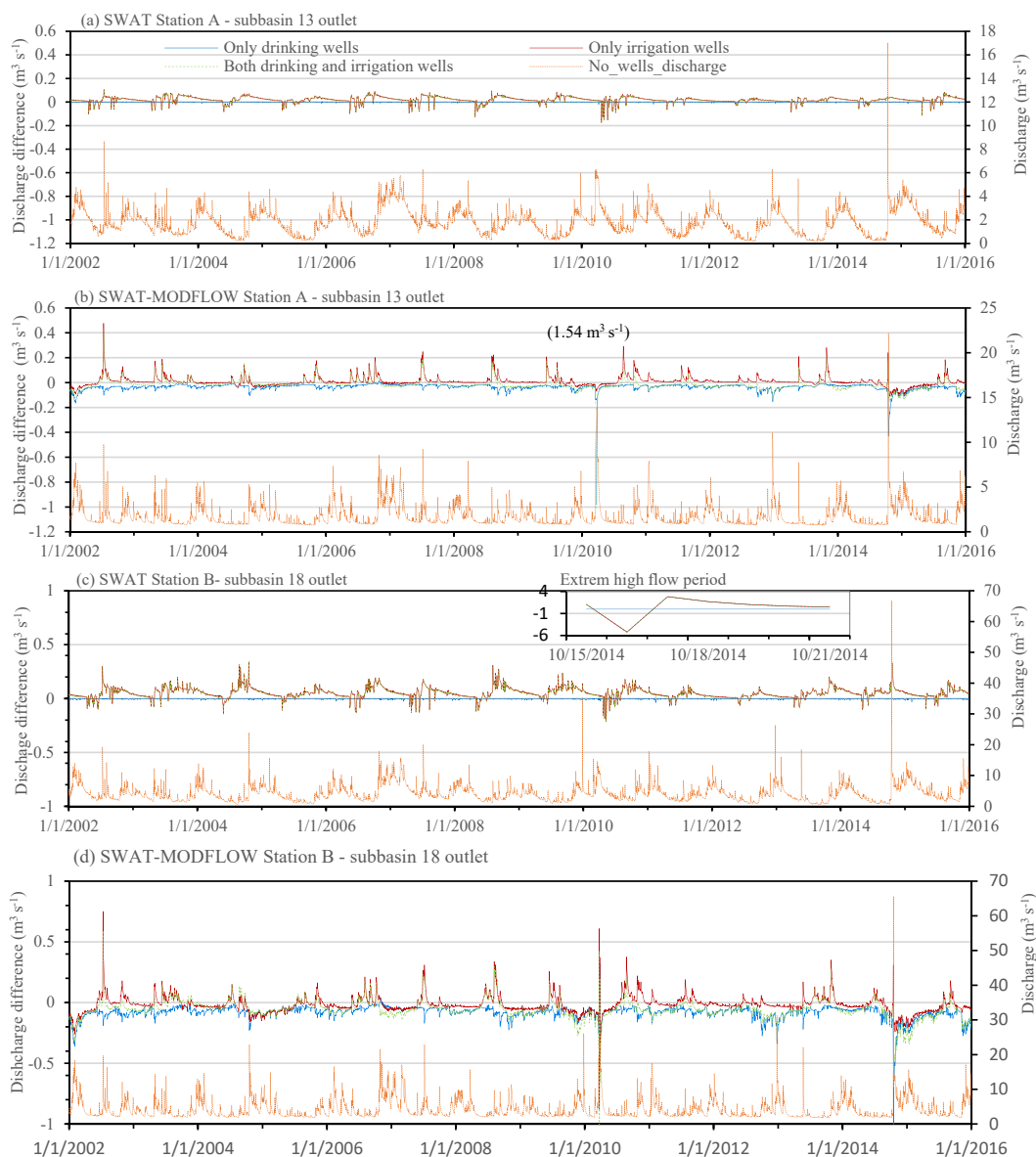


Figure 12. The simulated daily streamflow in the no-wells scenario and daily discharge differences between the abstraction scenarios (only drinking water wells, scenario 2; only irrigation wells, scenario 3; both drinking water and irrigation wells, scenario 4) and the no-wells scenario (scenario 1) at the outlets of subbasin 13 (station A) and subbasin 18 (station B) during the entire study period (2002–2015) based on SWAT and SWAT-MODFLOW, respectively. The value $1.54 \text{ m}^3 \text{ s}^{-1}$ in brackets is the streamflow difference between the no-wells scenario and the scenario with only drinking water wells on 24 March, 2010, which is outside the range of the plot area.

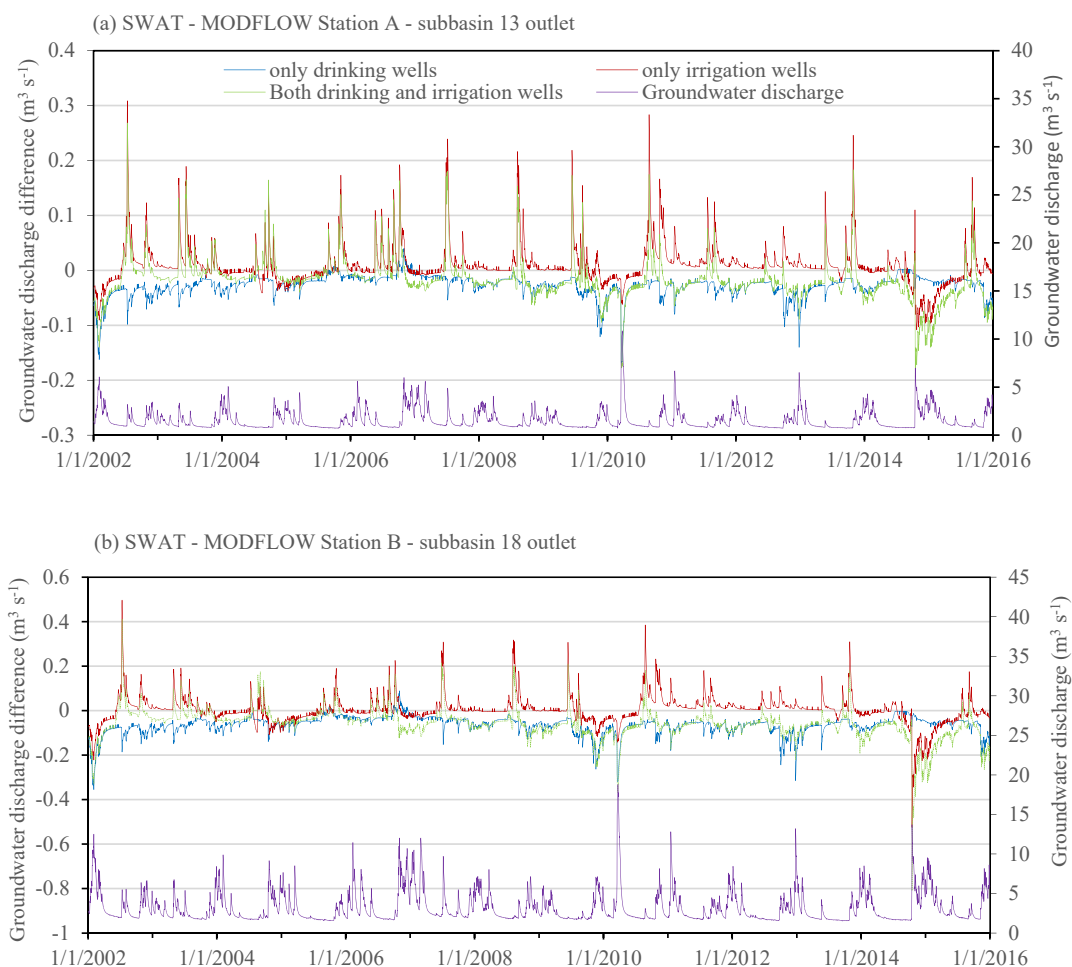


Figure 13. The hydrograph of simulated daily groundwater discharge to the stream network in the no-wells scenario and daily groundwater discharge differences between the abstraction scenarios (only drinking water wells, scenario 2; only irrigation wells, scenario 3; both drinking water and irrigation wells, scenario 4) and the no-wells scenario (scenario 1) in the upstream area of station A (a) and upstream area of station B (b), respectively, during the entire study period (2002-2015), based on SWAT-MODFLOW.